Chapter one

Introduction

The biliary tract, (biliary tree or biliary system) refers to the liver, gall bladder and bile ducts, and how they work together to make, store and secrete bile. Bile consists of waster, electrolytes, bile acids, cholesterol, and conjugated bilirubin. Some components are synthesized by hepatocytes (liver cells), the rest are extracted from the blood by the liver.

Bile is secreted by the liver into small ducts that join to form the common hepatic duct. Between meals, secreted bile is stored in the gall bladder. During a meal, the bile is secreted into the duodenum to rid the body of waste stored in the bile as well as aid in the absorption of dietary fats and oils.

A mathematical technique known as deconvolutional analysis was used to provide a critical and previously missing element in the computations required to quantitate hepatic function scintigraphically. This computer-assisted technique allowed for the determination of the time required, in minutes, of a labeled bilirubin analog (99mTc-disofenin) to enter the liver via blood and exit via bile. This interval was referred to as the mean transit time (MTT). The critical process provided for by deconvolution is the mathematical simulation of a bolus injection of tracer directly into the afferent blood supply of the liver.

HIDA (Hepatobiliary) scans very useful tool for evaluating the liver, gallbladder, and biliary system is called the Hepatobiliary (HIDA) scan. This scan demonstrates not only liver function, but also the function of the gallbladder. It is commonly used to diagnose abnormal function of the gallbladder. It also examines the gallbladder and the ducts leading into and out of the gallbladder. Many people have gallstones without ever having symptoms. However, these stones can cause acute abdominal pain by obstructing the gallbladder and the flow of bile. This is a very simple test to determine if gallbladder is obstructed. In this test the patient receives an intravenous

injection of a radioactive material called hydroxyiminodiacetic acid (HIDA). This material is taken up by the liver and excreted into the biliary tract. In a healthy person, this material will pass through the bile ducts and into the cystic duct to enter the gallbladder. It will also pass into the common bile duct and enter the small intestine, from which it eventually passes out of the body in the stool.

1.1 Anatomy of the liver

The liver is the largest organ of the human body (Figure 1.1), weighs approximately 1500 g, and is located in the upper right corner of the abdomen. The organis closely associated with the small intestine, processing the nutrient-enriched v nous blood that leaves the digestive tract. The liver performs over 500 metabolic functions, resulting in synthesis of products that are released into the blood stream(e.g. glucose derived from glycogenesis, plasma proteins, clotting factors and urea), or that are excreted to the intestinal tract (bile). Also, several products are storedin liver parenchyma (e.g. glycogen, fat and fat soluble vitamins).

Almost all blood that enters the liver via the portal tract originates from the gastrointestinal tract as well as from the spleen, pancreas and gallbladder. A secondblood supply to the liver comes from the hepatic artery, branching directly fromthe celiac trunc and descending aorta. The portal vein supplies venous blood underlow pressure conditions to the liver, while the hepatic artery supplies high-pressuredarterial blood. Since the capillary bed of the gastrointestinal tract already extractsmost O2 , portal venous bloo d has a low O2 content. Blood from the hepatic arteryon the other hand, originates directly from the aorta and is, therefore, saturated with o2 Bloo d from both vessels joins in the capillary bed of the liver and leaves via central veins to the inferior vein cava.

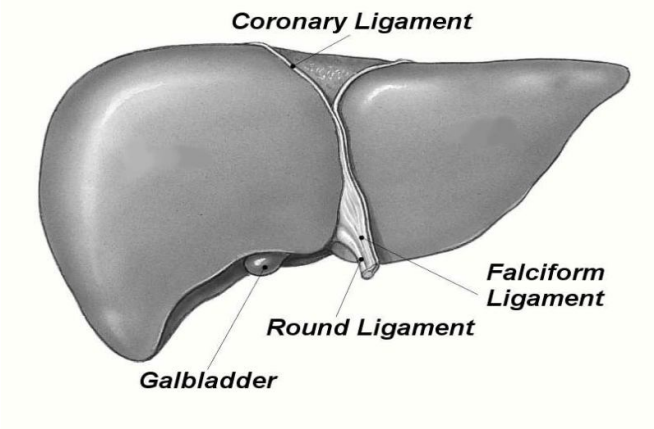

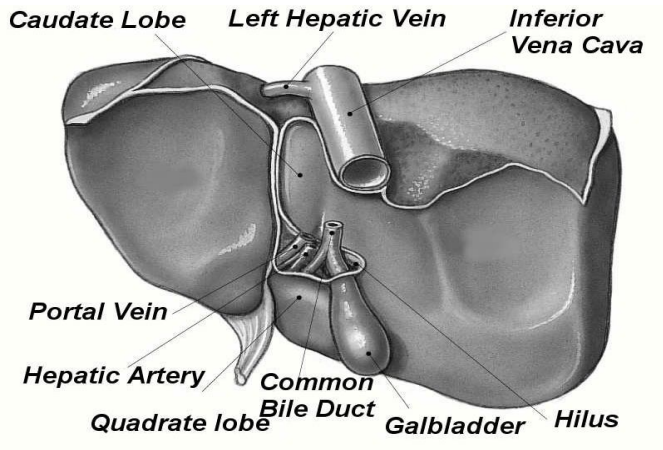

(Figure 1.1) the liver

1.1.1 Basic liver architecture

The major blood vessels, portal vein and hepatic artery, lymphatics, nerves andhepatic bile duct communicate with the liver at a common site, the hilus. Fromthe hilus, they branch and rebranch within the liver to form a system that travelstogether in a conduit structure, the portal canal (Figure 1.2). From this portalcanal, after numerous branching, the portal vein finally drains into the sinusoids,which is the capillary system of the liver. Here, in the sinusoids, blood from theportal vein joins with blood ow from end-arterial branches of the hepatic artery. Once passed through the sinusoids, blood enters the collecting branch of the central vein, and finally leaves the liver via the hepatic vein. The hexagonal structure with, defined as a lobule (Figure 1.3). The lobule largely consists of hepatocytes (livercells) which are arranged as interconnected plates, usually one or two hepatocytesthick. The space between the plates forms the sinusoid. A more functional unit ofthe liver forms the acinus. In the acinus, the portal canal forms the center anda the central veins the corners. The functional acinus can be divided into three zones: 1)the periportal zone, which is the circular zone directly around the portal canal, 2)the central zone, the circular area around the central vein, and 3) a midzonal area,which is the zone between the periportal and pericentral zone

1.1.2 Sinusoids

Sinusoids are the canals formed by the plates of hepatocytes. They are approximately 8-10μ m in diameter and comparable with the diameter of normal

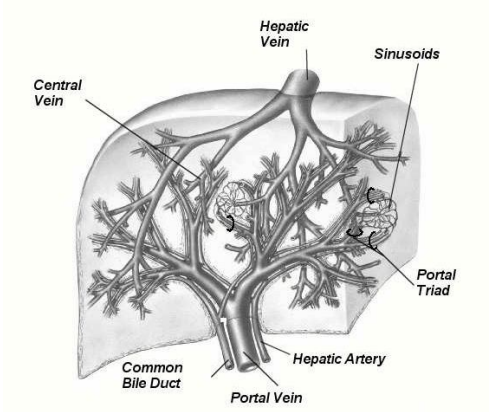

Figure 1.2: Network of branching and rebranchingbloo d vessels in the liver.

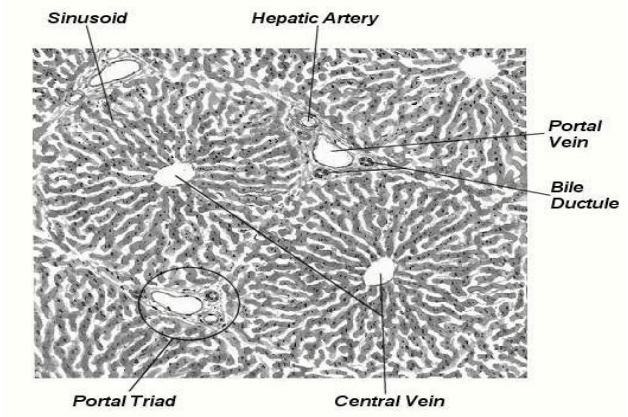

Figure 1.3: The liver lobule with portal canals (hepatic artery, portal vein and bileduct), sinusoids and collecting central veins.

Capillaries. They are orientated in a radial direction in the lobule. Sinusoids arelined with endothelial cells and Kuper cells, which have a phagocytic function.Plasma and proteins migrate through these lining cells via so-called fenestrations(100-150 nm) into the Space of Disse, where direct contact with the hepatocytesoccurs and uptake of nutrients and oxygen by the hepatocytes takes place. Onthe opposite side of the hepatocyte plates are the bile canaliculi situated (1μmμmdiameter). Bile produced by the hepatocytes empties in these bile canaliculi and is transported back towards the

portal canal into bile ductiles and bile ducts, and finally to the main bile duct and gallbladder to become available for digestive processes in the intestine. The direction of bile own is opposite to the direction of theblood own through the sinusoids.

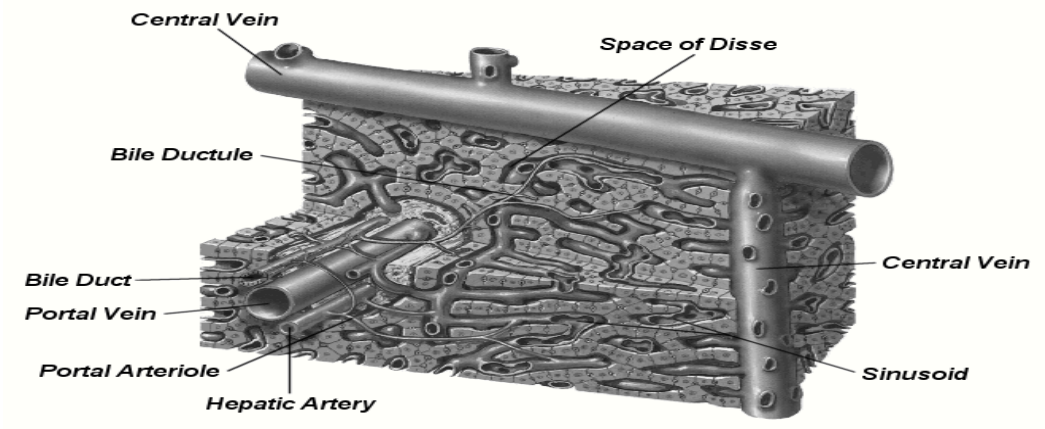

Figure 1.4: Detailed view of the liver sinusoidal structure.

1.1.3 Portal hepatic system

The liver receives nutrient-rich blood from the gastrointestinal tract via the portal hepatic system. The major vessel of this system is the portal vein, which is formed in the retroperitoneum by the union of the superior mesenteric and splenic veins, posterior to the neck of the pancreas. It passes obliquely to the right, posterior to the hepatic artery within the lesser omentum, and enters the liver at the portal hepatis. At the portal hepatis, the portal vein branches into right and left main portal veins that then follow the course of the right and left hepatic arteries. The right portal vein first sends branches to the caudate lobe, then divides into anterior and posterior branches that subdivide into superior and inferior branches to supply the right lobe of the liver. The left portal vein initially courses to the left, then turns medially toward the ligamentum teres. It branches to supply the lateral segments (segments II and III) of the left lobe and the superior and inferior segmental branches of segment IV.

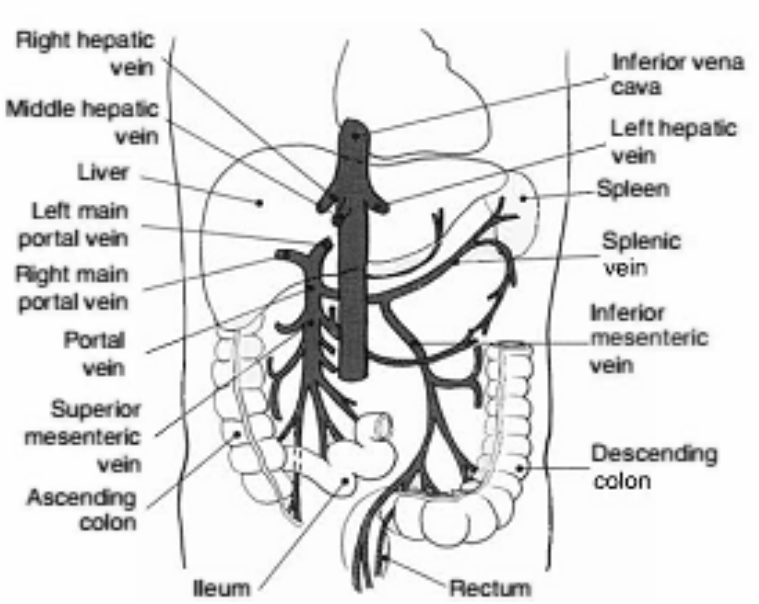

Figure1.5: Anterior view of portal hepatic system.

1.1.4 Gallbladder and biliary system

The biliary system is composed of the gallbladder and bile ducts (both intrahepatic and extrahepatic) that serve to drain the liver of bile and then store it until it is transported to the duodenum to aid in digestion (Figure 7.65). The hollow pearshaped gallbladder is located in the gallbladder fossa on the anteroinferior portion of the right lobe of the liver, closely associated with the main lobar fissure. It functions as the reservoir for storing and concentrating bile before being transported to the duodenum. The gallbladder can be divided into a fundus, body, and neck. The fundus is the rounded distal portion of the gallbladder sac that is frequently in contact with the anterior abdominal wall. The widest portion, the body, gently tapers superiorly into the neck. The narrow neck lies to the right of the porta hepatis and continues as the cystic duct. The neck contains circular muscles that create spiral folds within the mucosa that are called the spiral valves of Heister. These valves are especially

prominent at the bend formed by the neck and cystic duct, a common area for gallbladder impaction during acute or chronic cholecystitis. The gallbladder has a muscular wall that contracts when stimulated by cholecystokinin, forcing bile through the extrahepatic biliary system into the duodenum. Bile, formed within the liver, is collected for transport to the gallbladder by the intrahepatic bile ducts. The intrahepatic bile ducts run beside the hepatic arteries and portal veins throughout the liver parenchyma. The intrahepatic ducts mergeinto successively larger ducts as they follow a course from the periphery to the central portion of the liver, eventually forming the right and left hepatic ducts. The right and left hepatic ducts unite at the porta hepatis to form the proximal portion of the common hepatic duct (CHD), which marks the beginning ofthe extrahepatic biliary system. The CHD is located anterior to the portal vein and lateral to the hepatic artery in its caudal descent from the porta hepatis. As the CHD descends in the free border of the lesser omentum, it is joined from the right by the cystic duct to form the common bile duct (CBD). The CBD continues a caudal descent along with the hepatic artery and portal vein within the hepato duodenal ligament (Figure 7.65). It curves slightly to the right, away from the portal vein, then courses posterior and medial to the first part of the duodenum behind the head of the pancreas. The CBD follows a groove on the posterior surface of the pancreatic head, then pierces the medial wall of the second part of the duodenum along with the main pancreatic duct (duct of Wirsung) through the ampulla of Vater. The ends of both ducts are surrounded by the circular muscle fibers of the sphincter of Oddi.

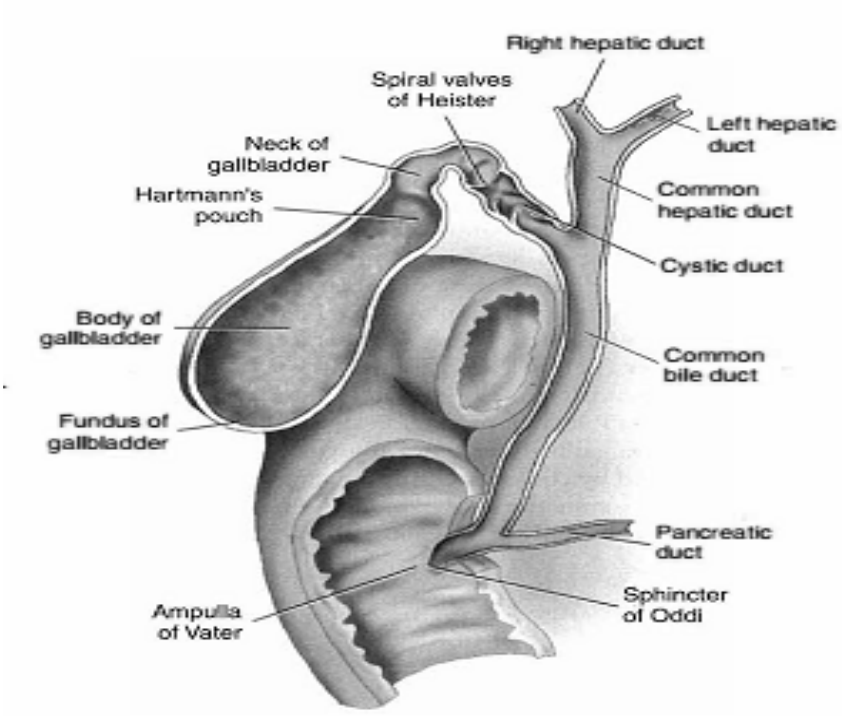

Figure 1.6: Gallbladder and biliary system.

1.2 Physiologyof the liver

1.2.1 Pressure distribution

Blood pressure in aerent vessels and pressure distribution inside the liver, is essentially similar for most species. Pressure in the hepatic artery, originating fromthe descending aorta and the celiac trunc, is considered to be the same as aortic pressure. This includes a high pulsatile pressure between 120 and 80 mmHg with frequency equal to the heart rate. Vessel compliance causes a gradual decreasein pulsation as the hepatic artery branches and rebranches inside the liver. Onceat the sinusoidal level, pulsation amplitude decreases to virtually zero and pressure drops to approximately 2-5 mmHg. On the other hand, pressure in the portal vein, originating from capillaries of the digestive tract, has no pulsation and a pressureof 10-12 mmHg. In the sinusoids, both portal venous and hepatic arterial pressureis 3-5 mmHg. Consequently, the

pressure drop inside the liver is much less in theportal venous system than in the arterial system. The pressure drop from the collecting central veins to the vena cava is then approximately 1-3 mmHg, actuatingslightly with respiration.

1.2.2 Flow distribution

Total human liver blood represents approximately 25% of the cardiac output, up to 1500 ml/min. Hepatic ow is subdivided in 25-30% for the hepatic artery (500 ml/min) and the major part for the portal vein (1000 ml/min). Assuming a human liver weighs 1500 g, total liver ow is 100 ml/min per 100 g liver. Comparing this normalized ow rate to other species, it can be concluded that total liver bloodow is 100-130 ml/min per 100 g liver, independent of the species. The ratio ofarterial: portal blood ow, however, is species-dependent. The hepatic artery originates directly from the descending aorta, and is therefore saturated with oxygen. It accounts for 65% of total oxygen supply to the liver. The hepatic artery alsoplays an important role in liver blood vessel wall and connective tissue perfusion It also secures bile duct integrity. The blood from the portal vein is full of nutrientsderived from the intestine and allows the hepatocytes to perform their tasks. Blood from the hepatic artery and the portal vein joins in the sinusoids. However, recent studies by others as well as our own observations, have revealed that there are bothcommon and separate channels for arterial and portal blood. The hepatic arteryperfuses the liver vascular bed in a ’spotty’ pattern, while the portal vein perfusesthe liver uniformly. The liver is able to regulate mainly arterial ow by means ofso-called sphincters, situated at the in- and outlets of the sinusoids. One of themost important triggers for sphincter function is the need for constant oxygen supply. If the rate of oxygen delivery to the liver varies, the sphincters will react andthe ratio of arterial: portal blood alters.

1.2.3 Physiology of Liver Preservation

Liver transplantation requires a period of preservation time, during which the liverafter explanation is stored and transported outside its natural environment. Thelength of this preservation or better bridging period from donor to recipient

dependson a large number of donor and recipient as well as logistical factors. Nowadays thistime zone is kept between 6-15 hours of preservation, while the liver is cut o fromits life sustaining mechanisms, i.e. bloo d ow and oxygen supply, and consequently, ischemic damage will occur. Three periods of ischemia are distinguished in a donorand transplantation procedure.

1. The first period is defined as the times in between clamping of the liver's aren't vasculature and start of the wash-out with ice-cold preservation solutionduring the pro curement phase in the donor. In this period of ischemia, blood to the liver is stopped and perfusion with the preservation solution viaa cannula takes place. During this period of ischemia the liver is still atbody temperature, for which reason this is called warm-ischemia. Duringthis warm-ischemic time, mainly damage to the hepatocytes occurs, and it istherefore very important to keep this period as short as possible. Especiallyin non-heart-beating donors (NHBDs) after cardiac arrest and awaiting thedonor operation and start of cold preservation, the warm-ischemic periodcan become too long, and result in a serious injury of hepatocytes with non function after transplantation

2. The second perio d of ischemia starts at the moment when the ice-cold preservation solution enters the microvasculature of the liver to wash-out the bloodA goo d wash-out of blo od cells is important to obtain optimal and uniformperfusion and co oling of the liver. Furthermore, remaining bloo d cells couldcause in ammatory reactions and trigger the immune response of the receiving patient against these donor cells. This cold ischemic period continuesduring the preservation period, in which the liver is transported to the recipient, and ends at the moment that the liver is taken out of its cold environment just prior to be placed in the 'warm' recipient's abdomen during the actual implantation. This second period takes place at 0-4 C, including the wash out with ice-cold solution and cold storage preservation period, and is definedas the period of cold ischemia. During this period of cold ischemia, not so much

hepatocytes, but more endothelial and biliary epithelial cells appear tobe injured

3. The last period of this bridging ischemia is the period needed to completethe vascular anastomoses during implantation. This procedure could take30-60 minutes, a period in which the liver lies in the abdominal cavity and isthus rewarmed by temperature of the bo dy. Once all vessels are connectedbetween donor organ and recipient vasculature, the liver is reperfused with blood and after the biliary anastomosis the transplantation is complete to minimize the impact of cold ischemic injury, two principal requirements forsuccessful preservation have to be considered: the temperatureact using hypothermia and the e act of the preservation solution Cooling the liver to hypothermic temperatures (0-4 C) lowers the rate ofmetabolism and the rate at which cellular components degrade. As a result, the need for nutrients and oxygen decreases and the organ can be preservedin a viable state for several hours.Although hypothermia is a key to successful preservation; it has negativeside e ects as well. The ma jor drawback of hypothermia is the induction ofcell swelling due to suppressed functioning of the cellular ion pumps. Thiscan be counteracted, however, by the use of an e active preservation solutioncontaining so-called impermeants, the use of intracellular-like solution andpossibly colloids. Another reason for using a specially developed preservation solution is to prevent ischemia-induced cellular acidosis, which requiresa powerful buer. Finally, in the initial reperfusion phase during transplantation the sudden increase in available oxygen (’respiratory burst’) results in the formation of toxic oxygen radicals. To counteract this last drawback, thepreservation solution should contain agents that are able to scavenge oxygenfree radicals

The combination of hypothermia and the use of an adequate preservation solution prevent hypothermic and preservation-induced injury, and make it possibleto keep the liver for a limited amount of time outside its physiologic environmentCold storage allows preservation for 12-15 hours in the clinics and even beyond 48hours in the

experimental setting. This time perio d is considered short to fulfillall requirements of an appropriate match between donor and recipient as well as ofcomplex logistic factors. Also, despite ma jor achievements in organ preservation, and especially in older donors, prolonged static cold storage is still accompanied byan increased primary non-function as well as reduced long term functional outcomeafter liver transplantation. To date, preservation times are kept short and any prolongation without a compromise to the viability of the liver would be a significantimprovement. Thus, hypothermic machine perfusion preservation could substantially increase the quality of preservation and lengthen the preservation period.

1.2.4Physiology of gallbladder

Each day, hepatocytes secrete 800–1000 mL (about 1 qt) of **bile,** a yellow, brownish, or olive-green liquid. It has a pH of 7.6–8.6 and consists mostly of water, bile salts, cholesterol, a phospholipid called lecithin, bile pigments, and several ions. The principal bile pigment is **bilirubin** (bil-i-ROO-bin). The phagocytosis of aged red blood cells liberates iron, globin, and bilirubin (derived from heme). The iron and globin are recycled; the bilirubin is secreted into the bile and is eventually broken down in the intestine. One of its breakdown products—**stercobilin** (ster-ko ¯-BI ¯-lin)—gives feces their normal brown color.

Bile is partially an excretory product and partially a digestive secretion. Bile salts, which are sodium salts and potassium salts of bile acids (mostly chenodeoxycholic acid and cholic acid), play a role in **emulsification** (e¯-mul-si-fi-KA ¯ shun), the breakdown of large lipid globules into a suspension of small lipid globules. The small lipid globules present a very large surface area that allows pancreatic lipase to more rapidly accomplish digestion of triglycerides. Bile salts also aid in the absorption of lipids following their digestion.

Although hepatocytes continually release bile, they increase production and secretion when the portal blood contains more bile acids; thus, as digestion and absorption

continue in the small intestine, bile release increases. Between meals, after most absorption has occurred, bile flows into the gallbladder for storage because the sphincter of the hepatopancreatic ampulla closes off the entrance to the duodenum. The sphincter surrounds the hepatopancreatic ampulla.

In addition to secreting bile, which is needed for absorption of dietary fats, the liver performs many other vital functions:

- ***Carbohydrate metabolism.*** The liver is especially important in maintaining a normal blood glucose level. When blood glucose is low, the liver can break down glycogen to glucose and release the glucose into the bloodstream. The liver can also convert certain amino acids and lactic acid to glucose, and it can convert other sugars, such as fructose and galactose, into glucose. When blood glucose is high, as occurs just after eating a meal, the liver converts glucose to glycogen and triglycerides for storage.
- ***Lipid metabolism.*** Hepatocytes store some triglycerides; break down fatty acids to generate ATP; synthesize lipoproteins, which transport fatty acids, triglycerides, and cholesterol to and from body cells; synthesize cholesterol; and use cholesterol to make bile salts.
- ***Protein metabolism.*** Hepatocytes *deaminate* (remove the amino group, NH2, from) amino acids so that the amino acids can be used for ATP production or converted to carbohydrates or fats. The resulting toxic ammonia (NH3) is then converted into the much less toxic urea, which is excreted in urine. Hepatocytes also synthesize most plasma proteins, such as alpha and beta globulins, albumin, prothrombin, and fibrinogen.
- ***Processing of drugs and hormones.*** The liver can detoxify substances such as alcohol and excrete drugs such as penicillin, erythromycin, and sulfonamides into bile. It can also chemically alter or excrete thyroid hormones and steroid hormones such as estrogens and aldosterone.

- ***Excretion of bilirubin.*** As previously noted, bilirubin, derived from the heme of aged red blood cells, is absorbed by theliver from the blood and secreted into bile. Most of the bilirubin in bile is metabolized in the small intestine by bacteria and eliminated in feces.
- ***Synthesis of bile salts.*** Bile salts are used in the small intestine for the emulsification and absorption of lipids.
- ***Storage.*** In addition to glycogen, the liver is a prime storage site for certain vitamins (A, B12, D, E, and K) and minerals (iron and copper), which are released from the liver when needed elsewhere in the body.
- ***Phagocytosis.*** The stellate reticuloendothelial (Kupffer) cells of the liver phagocytize aged red blood cells, white blood cells, and some bacteria.
- ***Activation of vitamin D.*** The skin, liver, and kidneys participate in synthesizing the active form of vitamin D.

Nuclear medicine occupies a unique niche amongst various imaging modalities by virtue of its ability to evaluate functional and physiologic parameters in a non-invasive and quantitative manner. Although at one time scintigraphic studies were used as primary modalities to address anatomic questions, these tasks are currently performed by the higher-resolution modalities ultrasound (US), computed tomography (CT), and magnetic resonance (MR) imaging. In current practice, nuclear medicine retains a more limited though unique role in the functional and physiologic characterization of tissue

In nuclear medicine clinical information is derived from observing the distribution of a pharmaceutical administered to the patient. By incorporating a radionuclide into the pharmaceutical, measurements can be made of the distribution of this radiopharmaceutical by noting the amount of radioactivity present. These measurements maybe carried out either in vivo or in vitro. In vivo imaging is the most common type of procedure in nuclear medicine, nearly all imaging being carried out with a gamma camera.

1.3Principle of nuclear medicine

Nuclear medicine imaging procedures differ from ordinary x-rays in that the gamma rays are emitted from the body rather than transmitted across the body, as in the case of x-rays. As in most modern imaging, the principle of tomography is used, that is, the person is viewed by radiation detectors surrounding the body, or by rotation of a gamma camera around the body. Small amount of radiopharmaceuticals is injected into vein, and its distribution at specific time periods afterward is imaged in certain organs of the body or in the entire body. The images are created by measuring the gamma-ray photons emitted from the organs or regions of interest within the body.

Within the solid gastrointestinal (GI) tract, colloid imaging of the liver visualizes the distribution of reticuloendothelial (RE) system cells which phagocytize intravascular particulate material from the blood while hepatobiliary scintigraphy evaluates the uptake and excretion of bile by hepatocytes. Specific radiopharmaceuticals such as 18F-FDG, 123I- or 131I-MIBG, 67Ga-gallium citrate and 111In-Octreotide are used to evaluate metabolic and receptor characteristics of tissues relevant to various pathological processes that affect the liver and spleen. Radiolabeled red blood cells (RBCs) are used to quantitate the blood flow and intravascular blood pool within the liver, thereby confirming the diagnosis of intrahepatic hemangioma.

1.3.1 Role of nuclearmedicineindiagnosis

The most important application of cholecystography is in the investigation of acute cholecystitis in patients with right upper quadrant pain,for which it has a higher sensitivity and specificity than ultrasound. Occasionally the early hepatic phase of the study may reveal unsuspected focal liver disease,such as abscess or metastases. In chronic cholecystitis ultrasound is the preferred initial investigation, in particular in the presence of obstructive jaundice and in biliary colic. However, when ultrasound is not conclusive it is advisable to evaluate gallbladder function with biliary scintigraphy using CCK, which is a more sensitive test for revealing gallbladder

dysfunction. Biliary scintigraphy is helpful to differentiate the different causes of neonatal jaundice (neonatal hepatitis and biliary atresia), in which case 24-hour images are necessary.

Other uses of biliary scintigraphy are to evaluate bile leakage, in particular following surgery and also in evaluating the biliary system following livertransplant. Scintigraphy in the only clinically satisfactory test for bile reflux. Various other tests using duodenal intubation have been proposed, but they are unpleasant for the patient. Reflux may be evident at gastroscopy, but the circumstances of the test cannot be described as physiological. HIDA reflux studies are sensitive to 1% of the amount injected refluxing into the stomach.

1.4 Biliary excretion

The initial indication for biliary scintigraphy, to evaluate the etiology of acute right upper quadrant pain, remains current today. A second and expanding indication for this technique is the non-invasive evaluation of bile flow to assess extravasation or obstruction in the post-surgical and post-traumatic patient.

1.4.1 Radiopharmaceuticals

Attributes of an ideal radiopharmaceutical for evaluation of bile flow include labeling with a radionuclide of favorable imaging and dosimetry characteristics, rapid liver extraction and transit into the biliary system, little or no absorption from the intestine, and minimal renal excretion .99mTc-labeled iminodiacetic acid (IDA) derivatives approach these ideal criteria. Typically 185 MBq (5 mCi) of the DISIDA (2, 6-diisopropylacetanilido-iminodiacetic acid) or BRIDA(bromo-2, 4, 6-trimethylacetanilido-iminodiacetic acid) analogues are used for biliary scintigraphy; the latter has an advantage of superior liver extraction and is therefore favored in patients with more severe hepatic dysfunction. While the IDA analogues generally resemble bilirubin in their uptake and excretion, they are not conjugated as is bilirubin.

1.4.2 Hepatobiliary Scintigraphy Technique

Ensuring an optimal scintigraphic result starts with proper patient preparation. It is well recognized that biliary flow and GB motility is a complex process that can be dramatically altered by a multitude of variables. Ideally, the patient is instructed to avoid opiates and opioid drugs and to fast for 4–24 h prior to the test. It is preferred that the last pre-test meal (abedtime snack) contains a significant fatty component if it can be tolerated by the patient. This would empty the GB, rendering it in the state of refilling at the start of scintigraphy the following morning .Our institutional routine hepatobiliary scintigraphy (HBS) includes an optional rapid blood flow (scintiangiography) phase, and a slower dynamic (hepatobiliary) phase. Optimal resolution and counting statistics can be obtained by acquiring images in a 128×128 matrix size. The framing rate for the scintiangiography phase is one frame per second for a total of 60 s, while the subsequent images are acquired at one frame per 15 s for 1 h. The flow is best viewed by re-framing the rapid phase into 3–5 s per displayed frame, while the slower dynamic phase is re-framed into 2–4 min per displayed frame. If further dynamic imaging is required, it is typically acquired and displayed similar to the hepatobiliary phase for as long as the intervention is planned to last. When the gallbladder is the focus of attention, such as in the case of a gallbladder ejection fraction (GBEF) study, a 25°–35° left anterior obliquity renders the best separation of GB from duodenal activity (Fig. 1.7). Individualization on the basis of initial imaging may be needed in those who may have unusual GB position (intrahepatic, verticalposterior, etc.). Some indications (such as bile leak) call for even longer static acquisitions and will be addressed later.While the activity is continuously changing during HBS, and thus violates the pre-requisite of the steady state distribution, single photon emission computed tomography (SPECT) could be acquired with special modifications to provide improved visualization of regional liver function and the biliary tree (Oppenheim and Krepshaw 1988). SPECT imaging of the parenchymal phase is rarely useful in clinical practice, but may be helpful in

delineating hepatocellular function of a small and deeply located liver lesion that cannot be appreciated on planar HBS (Steiner et al. 2003).

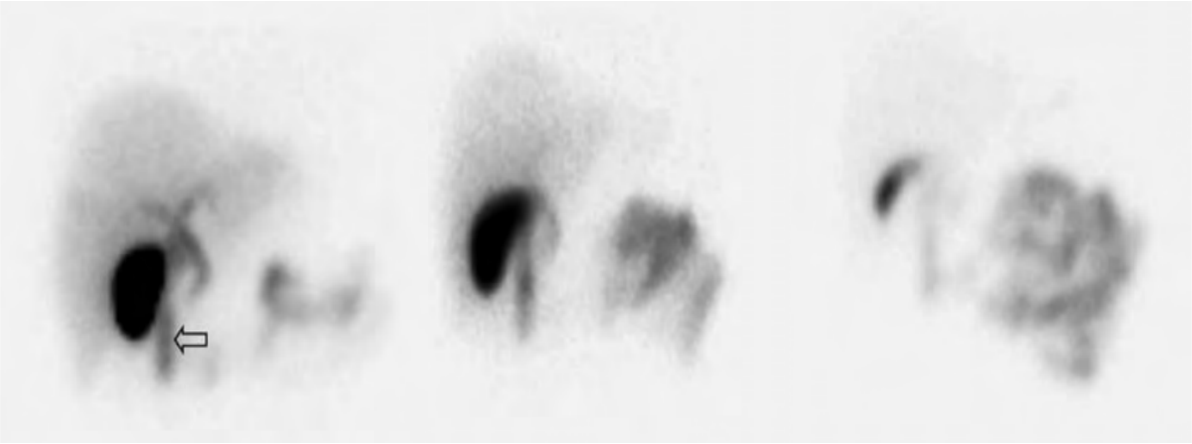

Figure 1.7:(a) show normal 60-min anterior image demonstrates a filled GB abutting the duodenal activity , (a) show the image corresponding to the trough GB activity at minute 24 from the start of CCK injection,(c) The image corresponding to the trough GB activity at minute 24 from the start of CCK injection.

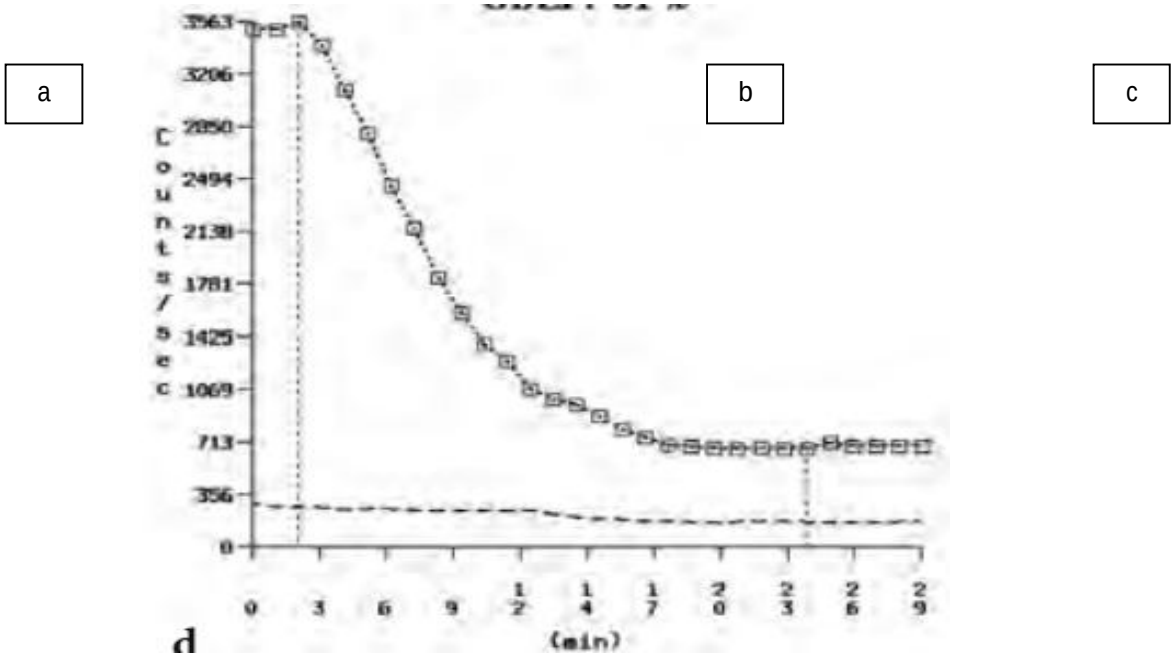

Figure 1.8 A normal curve following cholecystokinin.

1.4.3 Qualitative Assessment of HepatobiliaryScintigraphy

The scintiangiography phase may reveal gross abnormalities of the heart and the aorta, such as cardiomegaly or aneurisms (Stryker and Siegel1997). Liver blood flow via the hepatic artery is typically faint, as it represents only 25% of overall blood circulation through the organ. Activity in the liver .

Begins to accumulate more rapidly upon recirculation, as blood returns via the portal vein 3–5 s later. It is just before the portal phase that a focal blush signals a lesion with arterial hypervascularization, such as hepatocellular carcinoma, adenoma, or focal nodular hyperplasia. Conversely, decreased flow can be seen in hypovascular lesions exemplified by an abscess and a cyst (Yeh et al. 1973). Next is the hepatocellular or parenchymal imaging phase. The first 8-10 min of imaging offers a window into the functional hepatocellular integrity. Normally, the blood pool activity in the heart clears completely by the eighth minute (it may be faintly seen on the first 4-min image), with the tracer concentrated densely in the liver.

1.4.4 Quantitative Analysis in HepatobiliaryScintigraphy

By far the most common analytical application to HBS is quantitation of GBEF. It is the difference in GB counts, corrected by the background activity, between its maximal and minimal intensity, as a percent of the former. While a simple calculation, care should be taken to confirm that the GB region of interest (ROI) contains the GB throughout this imaging segment. It is common for the GB to change orientation, typically with the fundus moving in the cranial direction, assuming a more horizontal position. Such motion may cause a partial escape of GB outside the ROI, which is commonly drawn on the early image and applied to the entire image set, leading to an erroneously higher GBEF. Patient motion can have a similar effect by moving the GB outside a stationary ROI. An inappropriately positioned background ROI that includes bowel activity may occasionally lead to an erroneous

result. Another common problem with a stationary GB ROI is an unintentional inclusion of nearby bowel activity that moves into the ROItowards the end of the study. It is sometimes necessary to apply individual GB and background ROIs tothe pre-CCK and the image with least GB activity. All contemporary gamma camera systems offerquantitative GBEF as part of a standard package.Yet, some practitioners advocate visual (qualitative)assessment of images for characterization of gallbladder emptying (O'Neill and McCreath 2000).

In nuclear medicine practice today, however, it is difficult to find justification for omitting computerprocessing for GBEF in favor of visual inspection alone. A recent investigation advanced a mean GBEF(mGBEF) as a more reproducible measure of the organ's motility . It is defined as 100% minus the area under the time-activity curve, normalized to 100% and divided by the time interval from maximum to minimum counts per minute. While this parameter appears promising, testing it as a predictor of post-surgical success in patients with acalculous gallbladder disease is imperative prior to wide clinical acceptance.

A number of parameters are calculated from the time activity curves generated from the ROIs placed over the heart (activity in the circulation), liver, hepatic hilum, CBD, and duodenum. The whole liver activity curve analysis initially involved determination of time to the maximal activity (Tmax) and halftime of clearance (T1/2) from Tmax (Gilbert et al. 1987), which is a measure of bile formation and/or impedance to its flow. The normal Tmax is reached within 10 min of imaging, while the normal T1/2 for DISIDA and BromIDA are 18.8±2.5 min (Gilbert et al. 1987; Brown et al. 1988) and 16.8±1.3 min (Gilbert et al. 1987; Krishnamurthy and Krishnamurthy 1988), respectively. The hepatic activity washout, also called percent of radiotracer excreted, can be expressed by a percent clearance from Tmax to a specific time (typically at 30, 45, 60, and 90 min). This method is especially useful if an intervention is applied during the study to challenge the biliary dynamics ,Another clinically useful parameter of bile transit is the hepatic hilum to duodenum transit

time. It was found to be the most reproducible and the best discriminator between symptomatic and asymptomatic patients with sphincter of Oddi dysfunction .

Adding some complexity of deconvolutional analysis, the hepatic uptake of IDA compounds can be quantitatively expressed as extraction fraction . This parameter reflects functional hepatocellular integrity (100% in normal cases). In spite of usefulness in distinguishing hepatocellular disease from biliary problems, it is uncommonly used in contemporary practice. The gallbladder bile concentration function is amenable to scintigraphic analysis . Interestingly, it was shown to remain normal in chronic acalculousmcholecystitis. Whileadvancing our knowledge of GB physiology and pathophysiology, these methods are yet to find clinical utility.

1.4.5 Clinical Applications of HepatobiliaryScintigraphy

Acute Cholecystitis

ACC was the most common clinical application as HBS started to enter diagnostic practice. The initial useful criterion for a positive test was nonvisualization of radioactivity in the GB within 4 h of imaging. It was soon recognized that most false positive results were secondary to chronic cholecystitis .Several augmentations were developed to enhance specificity, including waiting for up to 24 h pre-treating patients with CCK (CCK pre-HBS), administering CCK after the first hour (CCKpost-HBS), and morphine augmented HBS . Morphine augmentation captured an overwhelming popularity in the contemporary practice. While similar in sensitivity to the 4-h HBS (96% versus 97%), it has significantly better specificity (84% versus 68%) for ACC . It also has better specificity than CCK preHBS .In a traditional approach the patient is imaged first for 1 h. If no GB activity is observed during that time, and other causes (recent meal, prolonged fasting, etc.) of non-visualization are excluded, the diagnoses to consider are either acute or chronic cholecystitis. Continued non-visualization during the 30 min following morphine injection establishes the former diagnosis, while appearance of the GB confirms the

latter one. Another variation of the technique is to inject morphine as soon as one observes activity in the small bowel . It may shorten the study considerably, but could limit the study's diagnostic ability for chronic cholecystitis.

Common Bile Duct Obstruction

Acute common bile duct (CBD) obstruction evolves through three main stages. During the initial 24 h the GB provides an overflow reservoir for the bile that cannot normally empty via the CBD. There is no dilatation of the biliary ducts, thus it commonly escapesdetection on anatomic imaging. HBS is done rarelyat this stage, but would typically show good liver uptake, visualization of the GB, and no activity in thebowel (Fig 1.8). After about 24 h, the GB compensation is overwhelmed and the biliary tree begins to distend. The back pressure shuts down the bile production, causing the "liver scan appearance" on HBS. This is the most typical finding in complete CBD obstruction, consisting of reasonably good hepatic extraction with no tracer transit into the GB, CBD or the bowel within 24 h of observation .Anatomic modalities would reveal CBD dilation. If the obstruction is not relieved in 96 h, the hepatocellular damage progresses with corresponding decrease in hepatic tracer uptake. Structural evaluation would often show progression of CBD dilation that extends to involve intrahepatic ducts. A common cause of false positive HBS for obstruction is severe cholestasis with or without hepatocellular dysfunction.

Unlike the thus far discussed complete CBD obstruction, diagnosing partial obstruction is much more complicated. Early studies established some basic principles. Usually, the intestinal activity is delayed, but observed within 24 h. One of the proposed criteria is a higher concentration of activity in the hepatic ducts or the common bile duct after 2 h, compared to liver activity (regardless of the gallbladder visualization). This pattern is not specific and may be seen in other hepatobiliary pathologies. Caution should be exercised in calling partial obstruction on the basis of scintigraphically apparent biliary duct dilation, as an increasing concentration of

radiotracer even in a normal size duct creates a “blooming” artifact . False positive studies can result after opioid administration , which can be clarified by reversing this effect with Naloxone . Further discussion on partial obstruction in postcholecystectomy sphincter of Oddi dysfunctioncan be found.

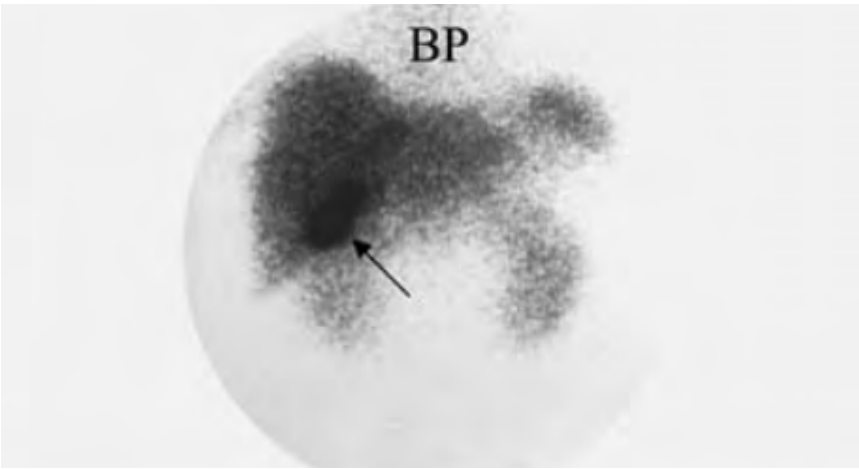

Figure 1.8: The image at 50 min revealed an unequivocal gallbladder filling with radioactive bile (arrow), but no activity in the bowel

Biliary Atresia

When the point of study is demonstration of biliary tree patency, increasing the bile flow (commonly achieved with phenobarbital or cholecystokinin) may become critical. It is especially important in differentiating biliary atresia from the neonatal hepatitis syndrome (severe intrahepatic cholestasis). For an optimal diagnostic result, these patients must be pretreated with a minimum of 3 (preferably 5–7) days of phenobarbital . The dosage is typically 5 mg/kg/day in divided doses, but it may need adjustment if the blood levels are subtherapeutic (below 15 mg/dl). Oral feeding is withheld for several hours before and up to 4 h after (duration of fasting depends on the clinical situation) the tracer injection to prevent dilution of biliary activity in the bowel. Delayed static views are obtained hourly for at least the first 6–8 h with an

additional view acquired for 10 min at 24 h (Fig.). A clear bowel activity excludes biliary atresia and the imaging can be stopped at that time. If bowel activity is not seen by 24 h, atresia is highly likely, but the child shouldbe further evaluated with cholangiogram, since some cases of severe cholestasis may cause a false positive study. Vicarious renal excretion can cause a false negative study – an avoidable situation when multiple views (anterior, posterior and left anterior oblique) are obtained to help sorting out the location of activity focus. Routine use of BromIDA is strongly recommended to reduce renal activity. The overall accuracy, sensitivity, and specificity of this technique for the diagnosis of biliary atresia are 91%, 97%, and 82%, respectively (Nadel 1996).

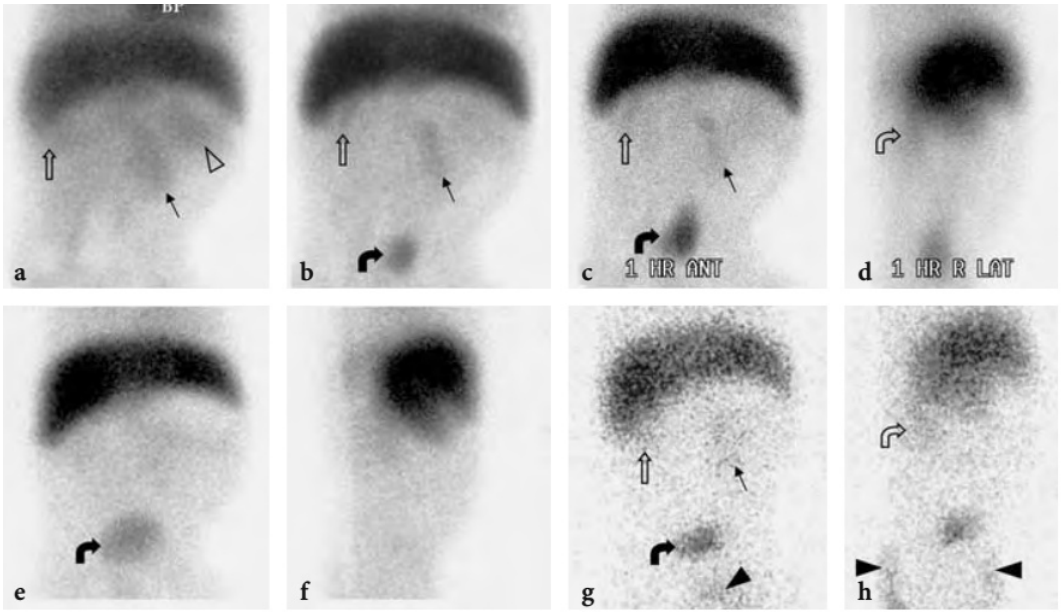

Figure 1.9: A 72-day-old infant boy with persistent jaundice demonstrates no biliary excretion on this 99mTc-mebrofenin study.

Gallbladder Hypokinesia Syndrome

There is a heterogeneous group of conditions that presents as a chronic, periodic abdominal pain, often biliary-like (“colicky”) in character, and united by a common

finding of gallbladder hypokinesia. First described and detailed utilizing cholecystokinin cholecystography it remains a highly debated and evolving entity . Because of complex mechanisms involved in GB contractile regulation its hypokinesia in response to CCK can be a reflection of a great variety of etiologies. Some of them originate in the GB itself, such as chronic calculous cholecystitis, chronic acalculous cholecystitis, and the cystic duct syndrome. Others are at various remote locations that can be as near as sphincter of Oddi dysfunction, or as remote as inflammatory bowel disease. While the former group is likely to benefit from cholecystectomy, the latter one is not. It is a daunting task for a clinician to identify patients in the latter group to avoid unnecessary cholecystectomy. The ability to exclude these patients, and thesubsequent ratio of the two groups within a study population, is what probably explains variability inthe reported power of CCK-GBEF to predict the relief of symptoms following cholecystectomy. A majority of studies report high predictive value of the test while a minority offers an opposing view . Diagnostic stimulation of GB contraction is presently a focus of some controversy in respect to the choice between the fatty meal and intravenous CCK. Standardization does not exist in either the composition of the former or the dosage of the latter. While the fatty meal would seem to be the most physiological approach, it is not studied specifically in thegallbladder dyskinesia population to determine its predictive value for relief of symptoms after surgery. However, there are well established normal values for some standardized fatty meals .The debate about CCK infusion rate is also unsettled and best exemplified in published argument exchanges. The only clinically validated slow infusion technique in adults involved administration over 45 min. It was observed that maximal GB contraction was achieved by 15 min into the infusion. Hence, an infusion over 15 min with image acquisition for 30 min seems to be most practical. There is a well established normal range for a total CCK dose of 0.02 µg per kilogram administered over 15 min . This dosage was later used successfully to predict response to cholecystectomy in children and adolescents with gallbladder hypokinesia syndrome . While GBEF of less than

35% is considered abnormal, some authors advocate a more liberal threshold of 50% . It is optimal to acquire images in 25º–35º left anterior oblique projection to prevent contribution of duodenal activity to the GB ROI. Application of GBEF in hospitalized patients who are typically unstable, undergoing some treatment, and often suffering from nausea, abdominal pain and other gastrointestinal symptoms, warrants a word of caution. It is likely that in such cases GBEF may be abnormal as a result of pharmacological hormonal, or neural influences, causing significant reduction in specificity of the test. Only a normal result under such circumstances would be clinically helpful. Therefore, experts recommend using this test in clinically stable outpatients only. For example, increased GB contractility is observed with cholinergic agonists erythromycin nonsteroidal anti-inflammatory drugs and those with vagotomy. These circumstances may promote false negative results, while false positive studies are more common and can result from reduced GB contractility secondary to narcotics, endotoxins associated with severe intercurrent illness and progesterone.

Post-Operative Applications

The most useful post-operative application of HBS is in patients with a suspected bile leak. Laparoscopic cholecystectomy is a common procedure with 1%–3% of early symptomatic bile leak. Interestingly, the incidence of asymptomatic self-resolving leak is about 7% (Hasl et al. 2001). The diagnosis is basedon extraluminal appearance of the bile. It can beseen in the gallbladder fossa (a “phantom gallbladder”), track along or around the liver, make its way to the paracolic gutter, or appear as a typical diffuse peritoneal distribution pattern. It is useful to keep in mind the typical normal pattern of tracer transit through the biliary and the bowel tracts in distinguishing the instances of extraluminal appearance. One can appreciate the rate of leakage, which would convey the clinical gravity. In our experience the voluminous leaks are unlikely to cease spontaneously. Chronic leaks may

misleadingly appear as a minimal activity and much later in the study, as the receiving biloma fills to its capacity. It is imperative in those instances to obtain up to 4-h delay images. In a sizable series from Case Western Reserve University the test's sensitivity and specificity was an impressive 100%, consistent with our institutional experience. While anatomic modalities can visualize intra-abdominal fluid collections, only HBS is able to definitively and noninvasively differentiate the bile leak from postoperative seroma, lymphocele, and hematoma. HBS is similarly diagnostic in other abdominal surgeries with potential for biliary leak or biliary fistula formation . HBS is helpful in the diagnostic evaluation of patients with postcholecystectomy abdominal pain, which is observed in 5%–60% of those patients. This heterogeneous group includes sphincter of Oddi dysfunction, cystic duct or GB remnants, and biliary tree obstruction or injury. It was initially suggested that sphincter of Oddi dysfunction may be diagnosed before cholecystectomy onCCK-HBS by observing a prominent CBD post-CCK (DeRidder and Fink-Bennett 1984). However, later reports showed that CCK-HBS is not useful for this indication. The accuracy of CCK augmented HBS for sphincter of Oddi dysfunction detection in postcholecystectomy patients was near perfect in some of the early reports. In a larger prospective series the test was found to correlate poorly with manometry (the reference standard). Encouragingly, the authors discovered that abnormal HBS in this population predicted those who gained sustained symptomatic relief after sphincterotomy. This observation was later confirmed in a larger series at another institution .The latter investigators used a practical measure of the hepatic hilum to the duodenum transit time. It becomes unimportant that incoming literature points out that this parameter correlates poorly with manometry , for it is able to predict which patient is likely to benefit from sphincterotomy and can do that better than manometry . Another useful approach to this group of patients is to augment HBS with morphine injection. An abnormally slow DISIDA clearance from the liver had about 80% sensitivity and specificity. On the other hand, acceleration of biliary tracer clearance from the liver by administering glyceryl

trinitrate is a useful approach to demonstrating sphincter of Oddi dysfunction and differentiating it from organic obstruction.Supposedly, the nitrate relaxes the tight sphincter of Oddi and allows for faster flow through the CBD. This recently introduced methodology is awaiting the ultimate evaluation by testing it for prediction of symptomatic relief or improvement after sphincterotomy. Other less frequent symptomatic complications after cholecystectomy where HBS is useful include the cystic duct or gallbladder remnants , billiard tree obstruction , and increased incidence of symptomatic biliary reflux into the stomach and esophagus.HBS plays an important role in the evaluation of liver transplant patients. The bile leak detection can be definitively diagnosed and localized in those without severe intrahepatic cholestasis. Vascular occlusion can be detected early on HBS by visualizing reduced or absent tracer uptake in an anatomically. While reducedhepatocellular function and cholestasis are nonspecific findings in rejection sequential HBS is helpful in assessing its response to therapy Transplant infarct is the final stage of rejection and would be scintigraphically indistinguishable from primary vascular occlusion, resulting in ominous “phantom liver” sign .

1.5 Research problems:

There is currently no reliable method to assess acute changes in gallbladder function. Must rely on clinical findings or measure changes in the level of substances metabolized by the liver .a process which involves a considerable time delay between cause and effect .in this study describe a scintigraphic technique coupled with a computer using quantification analysis.

1.6 Objective

The main objective of the study is to characterize liver scintigraphy objectively so as to over com the subjectively of the diagnosis.

1.6.1Specific objectives

- To measurement the count in the liver and gallbladder respect to the time.
- To calculate the absorption coefficient of liver and gallbladder uptake and secretion.
- To correlate between the liver and gallbladder uptake with patient condition.
- To illustration the function of liver and gallbladder.

1.7 Importance of study

In the presence of right upper quadrant pain, failure to visualize the gallbladder by 4 hours with normal passage of activity to the bowel is diagnostic of gallbladder disease (acute cholecystitis), and indicates cystic duct obstruction. While delayed visualization of the gallbladder usually indicates chronic cholecystitis, a more specific test would be to look at the response of gallbladder to CCK or fatty meal which will be compromised in this condition.

1.8 Overview of the study:-

- This study is consisted of five chapters, with chapter one is anintroduction about the liver disease and also would be concluded on general anatomy and physiology. Taken an over view about the method would be followed in this thesis.While chapter two gives a comprehensive literature review which include studies conducted to Characterization of hepatobiliary Scintigraphy using quantification analysis.Chapter three described the material used to collect the data and method the method followed in data collections. Chapter four include presentation of the results which include frequency tables and scatter plot and their dissection; finally chapter five includes a highlight the conclusions and further recommendations.

Chapter two
Literature review

Graafet et al. (2010) described assessment of future remnant liver function using hepatobiliary scintigraphy in patients undergoing major liver resection. 99mTc-mebrofenin hepatobiliary scintigraphy (HBS) was used as a quantitative method to evaluate liver function. The aim of their study was to compare future remnant liver function assessed by 99mTc-mebrofenin hepatobiliary scintigraphy with future remnant liver volume in the prediction of liver failure after major liver resection. The data was collected by Computed tomography (CT) volumetry and 99mTc-mebrofenin hepatobiliary scintigraphy were performed prior to major resection in 55 high-risk patients, including 30 patients with parenchymal liver disease. Liver volume was expressed as percentage of total liver volume or as standardized future remnant liver volume. Receiver operating characteristic (ROC) curve analysis was performed to identify a cutoff value for future remnant liver function in predicting postoperative liver failure. The result showed that Postoperative liver failure occurred in nine patients. A liver function cutoff value of 2.69%/min/m2 was calculated by ROC curve analysis. 99mTc-mebrofenin hepatobiliary scintigraphy demonstrated better sensitivity, specificity, and positive and negative predictive value compared to future remnant liver volume. Using 99mTc-mebrofenin hepatobiliary scintigraphy, one cutoff value suffices in both compromised and noncompromised patients. In the conclusions preoperative 99mTc-mebrofenin hepatobiliary scintigraphy is a valuable technique to estimate the risk of postoperative liver failure. Especially in patients with uncertain quality of the liver parenchyma, 99mTc-mebrofenin HBS proved of more value than CT volumetry.

Shah et al (2012)described utility of Tc99m-Mebrofenin hepato-biliary scintigraphy (HIDA scan) for the diagnosis of biliary atresia.. The aim of their study to determine the utility of Tc99m-Mebrofenin hepatobiliary scintigraphy (HIDA scan) for diagnosis of biliary atresia in patients with neonatal cholestasis. The data was collected byusing the retrospective analysis of 46 patients with neonatal cholestasis who underwent HIDA scans from May 2005 to July 2007. Biliary atresia (BA) was diagnosed on the basis of intra-operative cholangiogram. Non-BA patients were included in the neonatal hepatitis (NH) group. All patients received phenobarbitone and ursodeoxycholic acid for 5 days, prior to the HIDA scan. The HIDA scan was evaluated on the basis of uptake of the radioactive tracer by the liver at 5 minutes after intravenous injection; retention of radioactive tracer within the liver at 24 hours after injection and visualization of excretion of tracer into the intestine upto 24 hours after administration. The results of the HIDA scans were analyzed and correlated with the final diagnosis, gender and age of the patients. Chi-square test was employed for statistical analysis. The result showed that the age of presentation of our patients ranged from 5 days to 6 months. The male: female ratio was 37:9. Of the total 46 patients, 28 had BA and 18 had NH. All 28 (100%) patients diagnosed with BA showed persistent radiotracer in the liver at 24 hours whereas 17 (94.4%) of the 18 NH patients showed hepatic radiotracer retention ($p = 0.207$), the difference being statistically insignificant. Twenty two (78.6%) patients of BA showed no excretion of the radiotracer at 24 hours whereas only 7 (38.9%) of the NH group did not excrete the radiotracer ($p = 0.007$), which was statistically significant. Neither the sex nor the age of the child contributed to any difference on the hepatic retention ($p = 0.618$ and 0.235, respectively) or on the intestinal excretion ($p = 0.307$ and 0.9, respectively) of the radiotracer. In the conclusions HIDA scan is a useful tool for screening of biliary atresia in patients with neonatal cholestasis. Non excretion of the radioactive radiotracer into the intestines even after 24 hours of radiotracer administration can suggest biliary atresia in majority of patients.

3

Al Sofayan et al described nuclear imaging of the liver: is there a diagnostic role of HIDA in Posttransplantation. The aim of their study to detect early posttransplantation biliary complications. The data was collected by using 34 liver transplantations (recipients of mean SD age of 43.0 _ 15.7 years) were performed in 25 (73.5%) males from 20 (58.8%) cadaveric donors and 14 (41.2%) living-related donors. The subjects underwent HIDA scans using a single head gamma camera Meridian (Philips) after intravenous (IV) administration of 185 MBq Tc-99m Disofenin. The mean time _ SD posttransplantation to HIDA scan was 14.6 _ 18.2 days (range, 0–74). The results were compared with endoscopic retrograde cholangiopancreatography, magnetic resonant cholangiopancreatography, percutaneous cholangiograhy, and/or liver biopsy. The result showed that Twenty-four abnormalities were detected by HIDA scan in 16 patients (47.1%): 10 (29.4%) biliary leaks; 4 (11.4%) biliary obstruction or cholestasis; 1 (2.9%) delayed uptake; 5 (14.7%) delayed blood pool clearance; and 8 (23.5%) delayed transit to the bowel. The complications were more common among living-donor compared with deceased-donor graft recipients, albeit a not statistically significant difference (*P* _ .066). Total and direct bilirubin levels were significantly higher in patients with abnormal than normal HIDA scans (*P* _ .011 and *P* _ .040, respectively). The sensitivity and specificity of HIDA scans to detect overall postoperative complications were 100% and 66.7%, respectively. Biliary leak results were false positives in 7/10 patients, and true in 3. Detection of obstruction was 75% sensitive by HIDA. In the conclusions HIDA scans are a noninvasive, reliable modality for early exclusion of posttransplantation biliary complications. However, correlation with clinical status and imaging modalities is essential to confirm detected abnormalities.

GerbailandShakuntala (2003) described role of quantitative cholescintigraphy and ultrasound in early detection and patient management. The aim of their study was to find out the functional and morphologic changes that follow immediately after acute critical obstruction of the common bile duct. The data was collected by using eight patients who presented with acute onset of abdominal pain underwent clinical and biochemicalevaluation, along with morphological imaging with the ultrasound and functional imaging with Tc-99 mebrofenin (cholescintigraphy). Functional images were supplemented by quantitative measurement of hepatic extraction fraction (HEF) and excretion halftime (T1/2). All patients had confirmatory endoscopic retrograde cholangiopancreatography (ERCP) followed by sphincterotomy or stent insertion for relief of CBD obstruction. Post-therapy follow-up liver function tests were obtained .the result showed that at ERCP, all eight patients were found to have critical obstruction of the common bile duct, due to gallstones in four, and bile sludge or gravel in the other four. On admission, liver function tests showed mild elevation; CBD size was normal on ultrasound in all but one. Quantitative cholescintigraphy showed no bile formation during the first hour, and demonstrated marked prolongation of excretion halftime with relatively high HEF value in all. Sphincterotomy with extraction of stone or gravel relieved obstruction in seven, and one patient had CBD stent insertion followed by laparoscopic cholecystectomy. Liver function either improved or stabilized in all at discharge.in the Conclusion: Acute critical obstruction of the common bile duct is characterized clinically by sudden onset of abdominal pain, mild elevation of liver enzymes, normal size common bile duct, with high extraction of Tc-99m HIDA, but no excretion into bile. Combined use of liver functional tests, quantitative cholescintigraphy, and ultrasound examination provide enough information to justify the need for patient hospital admission, and an urgent ERCP for early relief of obstruction. This approach contributes for both early recovery of liver function and early patient discharge from the hospital.

Bennink et al (2003) described assessment of Postoperative Remnant Liver Function Using Hepatobiliary Scintigraphy. Hepatic resection is the therapy of choice for malignant and symptomatic benign hepatobiliary tumors. The concept of remnant liver volume (RLV) has been introduced and can be assessed with CT. However, inhomogeneous liver function distribution and a lack of correlation between morphologic hypertrophy and functional recovery fuelled the enthusiasm for functional imaging. The aim of the present study was to assess liver function reserve (LFR) and remnant liver function (RLF) before and after major liver surgery with hepatobiliary scintigraphy (HBS) and to compare scintigraphic results with volumetric CT data and indocyanine-green (ICG) clearance test results. Furthermore, HBS was used to assess functional recovery of liver function, and results were compared with volumetric data. The data was collected by using fifteen patients with a partial liver resection were included. HBS was performed before, 1 d after, and 3 mo after surgery. ICG clearance and CT were performed before and 3 month after surgery. Liver function determined with HBS was compared with ICG and volumetric data. The results showed that liver function determination using HBS was highly reproducible. A strong positive association (r _ 0.84) was found between LFR determined with HBS and ICG clearance. Little or no association (r _ 0.27) was found between CT volumetric analysis and corresponding ICG clearance. A strong positive association (r _ 0.95) was found between the RLF determined preoperatively on HBS and the actually measured value postoperatively. A weak positive association (r_0.61) was found between functional liver regeneration and liver volume regeneration in the 3 mo after partial liver resection. In the Conclusion: HBS offers a unique combination of functional liver uptake and excretion with the ability to assess the preoperative LFR and to estimate the RLF preoperatively. Determination of the RLF instead of the RLV might clarify some of the discrepancies observed in the literature between RLV and clinical outcome in patients with an inhomogeneous liver function. Finally, liver function regeneration can be monitored using HBS.

Onodera et al (2003) described assessment of hepatic functional reserve using 99mTc DTPA galactosyl human serum albumin SPECT to prognosticate chronic hepatic diseases validation of the use of SPECT and a new indicator. It is generally known that scintigraphy of 99mTc diethylenetriaminepentaaceticacidgalactosyl human serum albumin (99mTc-GSA) is useful for assessing hepatic functional reserve. For hepatic functional indicators, the index of the calculated planar image has been used in previous studies. However, there have been few reports that suggest that the indicators calculated from static SPECT data would be useful for the assessment of hepatic function. The aims of this study was to establish a simple method for assessing hepatic functional reserve using the liver SPECT of 99mTc-GSA and to apply this method for rich stratification in patients with chronic hepatic diseases. The data was collected by using a liver phantom (a 50% concentration of 99mTc solution) was used to compare the planar and SPECT methods. According to the definition of the new indicator, the liver SPECT of 99mTc- GSA was divided by a syringe SPECT of 99mTc-GSA and was called the liver uptake ratio (LUR). We correlated the LUR and the liver uptake ratio calculated according to the blood-sampling method. 99mTc-GSA SPECT was performed in 137 patients with hepatic diseases, including chronic hepatic diseases, and 20 healthy volunteers. The LUR was correlated between the formed subtypes for all subjects. The result showed thatthe acquired phantom-count ratio calculated by the SPECT method was more accurate than that acquired by the planar method. A good correlation was obtained between the LUR and the blood-sampling method ($r = 0.971$). The LUR was significantly lower in subjects with severe cirrhosis than in healthy subjects or those with chronic hepatitis and mild cirrhosis, and it was significantly lower in subjects with chronic hepatitis and mild cirrhosis than in healthy subjects. The LUR was significantly correlated with other hepatic function tests. Based on LUR, the chronic hepatic diseases were divided into two groups: Group A, with LURs 30% and higher, and Group B, with LURs below 30%. An LUR of 30% marked the 25th percentile of the mildcirrhosis group. The cumulative survival rates were lower in Group B than in Group A. in the Conclusion the SPECT method was superior to the planar method for assessing LURs. LUR was a suitable indicator of 99mTc-GSA clearance from the blood pool and of binding to the asialo-glycoprotein receptor. LUR is a simple and clinically useful indicator for the assessment of hepatic functional reserve in chronic hepatic diseases.

Seyed Mohsen et al (2015) described evaluation of cholestasis in Iranian infants less than three months of age. Cholestatic jaundice most probably occurs due to a pathological condition and the most frequent causes in early infancy are neonatal hepatitis and biliary atresia. Early diagnosis and treatment of infantile cholestasis can improve prognosis of liver diseases by prevention of the complications of these disorders The aim of this study was to find-out the possible etiologies in Iranian infants less than three months in Shiraz, South of Iran.the data was collected by using 122 infants under 3 months of age with cholestasis were studied in Nemazee Hospital (affiliated to Shiraz University of Medical Sciences) during the years 2001-2011. Demographic data, duration of jaundice, liver biopsy and the causes of cholestasis were recorded. The result showed that there were 76 males (62.3%) and 46 females (37.7%) with a mean age of 54.4 ± 23.7 days. The most common clinical finding was jaundice that was seen in all patients (100%).The onset of jaundice was the first day to the fifty two days of age, with an average age of 15.6 ± 16.1 days. Other findings included hepatomegaly in 92 patients (76.4%), clay-color stool in 54 (44.3%), and splenomegaly in 29 patients (23.8%). In this study, the most common causes of cholestasis were biliary atresia (30=24.6%), idiopathic neonatal hepatitis (30= 24.6%) and bile ducts paucity (16=10.3).In Conclusion The results of this study showed that biliary atresia and neonatal hepatitis are the most common causes of infantile cholestasis in this area. It is recommended that biliary atresia should be discriminated from other forms of neonatal cholestasis.

Yukio et al (2006) described Comparisons of the time-activity curves of the cardiac blood pool and liver uptake by 99mTc-GSA dynamic SPECT and measured 99mTc-GSA blood concentrations**.**The aim of their study was to determine the time-activity curve in the cardiac and hepatic region by 99mTc-GSA dynamic SPECT which is clinically used in liver scintigraphy and evaluate the temporal changes in the consistency and errors at the absolute scale using the regression equation of changes in the blood concentration of 99mTc-GSA. The data was collected by 11 patients who underwent99mTc-GSA dynamic SPECT over the 30 min period after IV

injection, the percentages of activity in the collected blood and in the blood pool estimated by dynamic SPECT were determined as the plasma clearance by blood collection and as the blood clearance by cardiac pooling. Extrahepatic uptake, expressesd as 100 − (% uptake in the liver by dynamic SPECT (%)) was calculated as the blood clearance by the liver. The regression equation ($Y = Y0 + Ae^{-\alpha t}$) was determined from the changes in the counts, expressed as a percent. Percent errors and the differences in the *Y*-intercept (*Y*0), coefficient (*A*) and slope (α) on the regression curve were compared. The result showed that blood pool clearance gradually exceeded the measured plasma clearance. The clearance by the liver started from a very low initial value and gradually became equal to that of plasma clearance over the first 15 minutes and exceeded it over the second 15 minutes. The *Y*-intercept was significantly higher in the blood pool clearance than that in the measured plasma clearance ($p < 0.001$), and the coefficient was significantly lower in the former than the latter ($p < 0.001$). The coefficient and slope were significantly lower in the hepatic clearance than the plasma clearance ($p < 0.001$, $p < 0.005$). In theconclusionsThe time-activity curve of the blood pool showed a tendency towards overestimation in the second half of the examination, probably due to scatter effect from the liver. The time-activity curve of liver uptake showed a tendency towards overestimation in the first half of the examination, probably due to the high concentration in the hepatic blood pool, and underestimation in the second half.

Cecilia Diana et al (2011) described The non-conventional use of 99mTc-Tetrofosmine for dynamic hepatobiliary scintigraphy. Classic dynamic hepatobiliary scintigraphy (DHBS) is commonly performed with 99m*Tc*-Iminodiacetic Acid(IDA) derivatives and represents a non-invasive diagnosis method for biliary dyskinesia, fistulas, surgical anastomosis.The aim of their study was to assesses the possibility of performing DHBS with 99m*Tc*-Tetrofosmine (TF), a radiopharmaceutical (RF) dedicated to myocardial perfusion scintigraphy (MPS), but being excreted through the liver. The possibility to use 99m*Tc*-TF for DHBS may be important in situations when the standardized RF for this procedure (IDA derivatives) is not available. The

data was collected by performed DHBS for 30 patients referred for investigation by internal medicine and surgery departments. The patients had been fasting for12 hours. The dynamic investigation started simultaneously with the intravenous (IV) administration of 37–110 MBq (1–3 mCi) 99m*Tc*-TF. Dynamic images were recorded for 30–45 minutes, one image per minute, followed by static scintigraphy at 1 h, 1.5 h, 2 h, and 3 h after IV injection. The result showed that The quality of scintigraphic images of the liver and biliary tree obtained at DHBS with **9**9m*Tc*-TF ensured the correct diagnosis of biliary dyskinesia, stasis, stenosis, and fistulas.In the conclusionsDHBS using **9**9m*Tc*-TF is justified by the image quality and by the good cost/benefits ratio. Because the IDA derivatives are not always available, this finding may be important for medical practice. **9**9m*Tc*-TF evacuated through the bile duct allows DHBS interpretation, while the necessary dose is approximately 8 to 20 times smaller than that used for myocardial perfusion scintigraphy**.**

Ira Shah et al (2012) described the utility of Tc99m-Mebrofenin hepato-biliary scintigraphy (HIDA scan) for the diagnosis of biliary atresia. The aim of their study was to determine the utility of Tc99m-Mebrofenin hepato-biliary scintigraphy (HIDA scan) for diagnosis of biliary atresia in patients with neonatal cholestasis. The data was collected by involves the retrospective analysis of 46 patients with neonatal cholestasis who underwent HIDA scans at the Pediatric Hepatobiliary Clinic, BJ Wadia Hospital for Children from May 2005 to July 2007. Biliary atresia (BA) was diagnosed on the basis of intra-operative cholangiogram. Non-BA patients were included in the neonatal hepatitis (NH) group. All patients received phenobarbitone and ursodeoxycholic acid for 5 days, prior to the HIDA scan. The HIDA scan was evaluated on the basis of uptake of the radioactive tracer by the liver at 5 minutes after intravenous injection; retention of radioactive tracer within the liver at 24 hours after injection and visualization of excretion of tracer into the intestine upto 24 hours after administration. The result showed that the HIDA scans were analyzed and correlated with the final diagnosis, gender and age of the patients. Chi-square test was employed for statistical analysis. Results: The age of presentation of our patients

ranged from 5 days to 6 months. The male: female ratio was 37:9. Of the total 46 patients, 28 had BA and 18 had NH. All 28 (100%) patients diagnosed with BA showed persistent radiotracer in the liver at 24 hours whereas 17 (94.4%) of the 18 NH patients showed hepatic radiotracer retention (p=0.207), the difference being statistically insignificant. Twenty-two (78.6%) patients of BA showed no excretion of the radiotracer at 24 hours whereas only 7 (38.9%) of the NH group did not excrete the radiotracer (p=0.007), which was statistically significant. Neither the sex nor the age of the child contributed to any difference on the hepatic retention (p=0.618 and 0.235, respectively) or on the intestinal excretion (p=0.307 and 0.9, respectively) of the radiotracer. Conclusion: HIDA scan is a useful tool for screening of biliary atresia in patients with neonatal cholestasis. Non excretion of the radioactive radiotracer into the intestines even after 24 hours of radiotracer administration can suggest biliary atresia in majority of patients.

Roelof J. et al (2015). described of postoperative remnant liver function using hepatobiliary scintigraphy. Hepatic resection is the therapy of choice for malignant and symptomatic benign hepatobiliary tumors. The concept of remnant liver volume (RLV) has been introduced and can be assessed with CT. However, inhomogeneous liver function distribution and a lack of correlation between morphologic hypertrophy and functional recovery fuelled the enthusiasm for functional imaging. The aim of their study was to assess liver function reserve (LFR) and remnant liver function (RLF) before and after major liver surgery with hepatobiliary scintigraphy (HBS) and to compare scintigraphic results with volumetric CT data and indocyanine-green (ICG) clearance test results. Furthermore, HBS was used to assess functional recovery of liver function, and results were compared with volumetricdata. The data was collected by fifteen patients with a partial liver resection were included. HBS was performed before, 1 d after, and 3 moafter surgery. ICG clearance and CT were performed before and 3 mo after surgery. Liver function determined with HBS was compared with ICG and volumetric data. The result showed that Liver function

determination using HBS was highly reproducible. A strong positive association (*r* _ 0.84) was found between LFR determined with HBS and ICG clearance. Little or no association (*r* _ 0.27) was found between CT volumetric analysis and corresponding ICG clearance. A strong positive association (*r* _ 0.95) was found between the RLF determined preoperatively on HBS and the actually measured value postoperatively. A weak positive association (*r*_0.61) was found between functional liver regeneration and liver volume regeneration in the 3 mo after partial liver resection.in the Conclusion HBS offers a unique combination of functional liver uptake and excretion with the ability to assess the preoperative LFR and to estimate the RLF preoperatively. Determination of the RLF instead of the RLV might clarify some of the discrepancies observed in the literature between RLV and clinical outcome in patients with an inhomogeneous liver function. Finally, liver function regeneration can be monitored using HBS.

K. Riyad et al (2007) Described the role of technetiumlabelledhepatoiminodiacetic acid (HIDA) scan in the management of biliary pain.The aim of their study was to assess the outcome of laparoscopic cholecystectomy on the basis of an abnormal provocative technetiumlabelled hepatoiminodiacetic acid (HIDA) scan for patients with typical biliary pain and normal transabdominalultrasound (TUS) scan. Prospective data were collected for 1201consecutive patients with typical biliary symptoms. Patients who were found to have a normal TUS and upper GIendoscopy subsequently underwent cholescintigraphy (HIDA scan). Patients with an abnormal HIDA scan, i.e.<40% ejection fraction with Sincalide® (cholecystokinin octapeptide) – were offered cholecystectomy. Symptomsand histology were reviewed postoperatively. The results showed thatin all, 48/1201 (4%) patients with typical biliary symptomshad a normal ultrasound and endoscopy; 35/48 patients had an abnormal provocative HIDA scan and allunderwent laparoscopic cholecystectomy. Histology in all cases revealed chronic cholecystitis and 18 patients hadsludge or microlithiasis within the gallbladder. At 6weekfollowup,31 of the 35 patients were completelyasymptomatic or improved. Furthermore, 79% of patients remained

symptomfreeor improved at a median followupof 28.5 months (range 4–70). In the conclusions HIDA scan is a useful clinical tool as an adjunct to the diagnosis andmanagement of patients who present with typical biliary pain and a normal TUS scan.

Graaf et al (2010).Described of hepatic function and liver functional volume before partial hepatectomy.Preoperative evaluation of future remnant liver (FRL) function is crucial in the determination of whether a patient can safely undergo liver resection. dynamic 99mTc-mebrofenin hepatobiliary scintigraphy (HBS) is used to measure future remnant liver FRL function, 2-dimensional planar images lack the ability to assess segmental liver function. Modern SPECT/CT cameras combine dynamic 99mTc-mebrofenin HBS with additional SPECT and the anatomic information of the CT scan. The aim of their study was to evaluate the additional value of 99mTc-mebrofenin SPECT for the measurement of segmental liver function and liver functional volume. The data was collected by preoperative CT volumetry and 99mTc-mebrofenin HBS with SPECT were performed in 36 patients undergoing liver resection. In 18 patients, postoperative 99mTc-mebrofenin HBS with SPECT was performed within 3 d after operation. Dual-head dynamic acquisitions were used to calculate FRL function using anterior and geometric mean (Gmean) datasets. Total and FRL functional liver volumes were measured by SPECT. the results showed that because the anatomic position of the liver, the anterior projection resulted in an underestimation of FRL function in patients undergoing left hemihepatectomy. In patients with normal liver parenchyma, total functional liver volume was comparable to total liver volume measured by CT volumetry, indicating that 99mTc-mebrofenin SPECT is an accurate method to measure hepatic volume. In compromised livers, compared with normal livers, FRL function per cubic centimeter of liver volume was significantly less. In addition, liver function was not distributed homogeneously, with the segments to be resected relatively more affected. FRL function, measured by a combination of SPECT and dynamic HBS, was able to accurately predict actual postoperative remnant liver function. in Conclusion the Gmean dataset is

recommended for the assessment of hepatic function by dynamic planar 99mTc-mebrofenin HBS. The combination of SPECT data with the dynamic uptake function measured by planar HBS provides valuable visible and quantitative information regarding segmental liver function and is an accurate measure for FRL function.

Col SS et al (2006) described hepato-biliary Scintigraphy in diagnosis of biliary atresia the aim of their study was to differentiation of biliary atresia BA from other causes of persistent neonatal jaundice . The data was collected by 14 infants (8 boys and 6 girls) had undergone Hepato-biliary scans. Age at investigation ranged from 41 days to 6months ,All patients underwent clinical examination,biochemical tests (including Liver Function Tests) and abdominal USG before Scintigraphy. Each patient was given an intravenous injection of 37 MBq99m Tc-Mebrofenin. Imaging was carried out on a Single Head Gamma Camera using a high resolution collimator with the patient in supine position. The results showed that Per-operative cholangiogram was carried out on all 14 patients. Biliary flow seen in 3 scintigraphic false positive cases (21%) was due to Bile Plug Syndrome. The remaining 11 (79%) in whom bile flow was not visualized during operative cholangiography were operated upon and hepato portoenterostomy performed. In conclusion prompt and accurate diagnosis of EHBA is of utmost importance in neonates as the success of surgical procedure is inversely related to age. Mebrofenin hepato-biliary scintigraphy is a simple, noninvasive and accurate diagnostic tool for suspected biliary atresia.

Sevilla et al (2007) described Hepatobiliary Scintigraphy With SPECT in Infancy .Hepatobiliary scintigraphy (HBS) is an important investigation for the diagnosis of biliary atresia (BA) and its differentiation from causes of conjugated hyperbilirubinemia that do not require surgical intervention. Delayed imaging at 24 hours and phenobarbitone augmentation for 5 days has been required to achieve high sensitivity and specificity with current techniques. The aim of their study was to explores whether adding single photon emission computed tomography (SPECT) performs as well as existing methods without requiring delayed 24-hour imaging and whether the phenobarbitone premedication is necessary in all cases. The data was collected by a retrospective analysis of 105 HBS studies on 94 patients was performed. HBS included SPECT at 4 to 6 hours postinjection when no tracer was seen in the gastrointestinal tract in the first 60 minutes. This was done in 80 patients. The result showed that gastrointestinal activity was seen in 14 patients within 60 minutes. For 4- to 6-hour studies, standard HBS and HBS with SPECT data showed a sensitivity of 100% for the diagnosis of BA. The specificity, accuracy, and positive likelihood ratios (PLR) were 67%, 75%, and 3 (confidence interval [CI] = 2.03–4.16) for planar imaging at 4 to 6 hours and 90%, 93%, and 10 (CI = 4.42–19) for 4- to 6-hour planar and SPECT imaging. When the 11 patients who had phenobarbitone stimulation were included, the results improved to 97%, 98%, and 30 (CI = 7.06–80). In conclusion the addition of SPECT 4 to 6 hours postinjection of tracer significantly improves the diagnostic accuracy of hepatobiliary scintigraphy compared with planar imaging alone. This accuracy is as good as HBS performed after phenobarbitone stimulation. The combined technique of HBS with SPECT and phenobarbitone has the highest accuracy. Delayed imaging at 24 hours is usually not necessary.

Wilmar etal (2010) described assessment of Hepatic Function and Liver Functional Volume Before Partial Hepatectomy Preoperative evaluation of future remnant liver (FRL) function is crucial in the determination of whether a patient can safely undergo liver resection. Although dynamic ^{99m}Tc-mebrofenin hepatobiliary scintigraphy (HBS) is used to measure FRL function, 2-dimensional planar images lack the ability to assess segmental liver function. Modern SPECT/CT cameras combine dynamic ^{99m}Tc-mebrofenin HBS with additional SPECT and the anatomic information of the CT scan. The aim of their study was to evaluate the additional value of ^{99m}Tc-mebrofenin SPECT for the measurement of segmental liver function and liver functional volume. The data was collected by Preoperative CT volumetry and ^{99m}Tc-mebrofenin HBS with SPECT were performed in 36 patients undergoing liver resection. In 18 patients, postoperative ^{99m}Tc-mebrofenin HBS with SPECT was performed within 3 d after operation. Dual-head dynamic acquisitions were used to calculate FRL function using anterior and geometric mean (Gmean) datasets. Total and FRL functional liver volumes were measured by SPECT .the results showed thatthe anatomic position of the liver, the anterior projection resulted in an underestimation of FRL function in patients undergoing left hemihepatectomy. In patients with normal liver parenchyma, total functional liver volume was comparable to total liver volume measured by CT volumetry, indicating that^{99m}Tc-mebrofenin SPECT is an accurate method to measure hepatic volume. In compromised livers, compared with normal livers, FRL function per cubic centimeter of liver volume was significantly less. In addition, liver function was not distributed homogeneously, with the segments to be resected relatively more affected. FRL function, measured by a combination of SPECT and dynamic HBS, was able to accurately predict actual postoperative remnant liver function .In conclusion the Gmean dataset is recommended for the assessment of hepatic function by dynamic planar ^{99m}Tc-mebrofenin HBS. The combination of SPECT data with the dynamic uptake function measured by planar HBS provides valuable visible and quantitative information regarding segmental liver function and is an accurate measure for FRL function.

Robert et al (2013) described Tc-99m Mebrofenin Hepatobiliary Scan in Obstructive Hepatobiliary Disease. Hepatobiliary radionuclide imaging is typically performed to assess for acute or chronic cholecystitis. The aim of their study was to retrospectively evaluate the role of delayed hepatobiliary imaging in patients with an obstructive pattern in determining IH or EH causes. The data was collected by using twenty-four patients met these criteria including 7 men and 17 women; aged 25-77 years (mean age, 52 years). all patients with both an initial and delayed Tc-99m mebrofenin hepatobiliary scan that demonstrated an obstructive pattern on initial 1 h of imaging during this time period. The average time interval for the delayed images measured from radiotracer injection time until image completion was 11.4 h with a range between 4 and 30 h . The result showed that a total of 24 patients demonstrated an obstructive pattern on Tc-99 m mebrofenin hepatobiliary imaging , The causes of IH obstruction consisted of hepatitis with the majority of the causes due to choledocholithiasis (n = 11). Other causes include common bile duct stricture (n = 2), cholangitis (n = 1) and biliary fistula (n = 1). In the conclusion the hepatobiliary imaging was only useful in uncovering bile obstruction that may not have been suspected clinically. Most notably, although evaluating for gallbladder disease was usually the clinical indication for the hepatobiliary scan, determining the presence of cholecystitis was severely limited since the obstructive pattern obscured the results.

Kevin J. Gaskin et al (1988) described liver disease and common bile duct stenosis in cystic fibrosis. The aim of their study was to determine the incidence of common-bile-duct lesions and their relation to liver disease in cystic fibrosis . the data was collected by we performed hepatobiliary scanning in 50 of 61 patients with cystic fibrosis who had hepatomegaly, abnormal liver function, or both and in 31 of 92 patients with cystic fibrosis who did not have hepatomegaly or abnormal liver function. The result showed that Ninety-six percent of the patients with liver disease had evidence of biliary tract obstruction, which was defined cholangiographically as a stricture of the distal common bile duct in the majority of cases. All the patients

without liver disease had normal intrahepatic and common-duct excretion of tracer. Abdominal pain was significantly more common in patients with common-duct obstruction (P<0.001), and enlarged gallbladders occurred only in such patients. Since fasting levels of serum bile acids were elevated in nearly half these patients, irrespective of the severity of their liver disease, serum bile acids may be markers of the severity of the common-duct lesion. In the conclusion that strictures of the distal common bile duct are common in patients with cystic fibrosis and liver disease. This association requires further study, since surgical relief of common-duct obstruction may prevent or ameliorate the hepatic complications of cystic fibrosis.

Spivak W et al (1987) described utility of hepatobiliary scintigraphy with 99mTc-DISIDA in neonatal cholestasis. We retrospectively evaluated the utility of hepatobiliary scintigraphy and various clinical factors in differentiating intrahepatic cholestasis from biliary atresia in 28 consecutive infants with neonatal cholestasis. One millicurie of technetium-labeled diisopropyliminodiacetic acid (DISIDA) was administered intravenously, and images were obtained for up to 24 hours or until gastrointestinal excretion was noted. Nine separate studies in seven infants with biliary atresia were correctly interpreted as showing no gastrointestinal excretion of radionuclide. Of the 21 patients with intrahepatic cholestasis, only nine had gastrointestinal excretion on the first study; in eight without excretion, a second study was done, and five of these showed gut excretion. All infants with either neonatal hepatitis (six) or inspissated bile syndrome (three) had demonstrable gastrointestinal excretion either on the first or second DISIDA study. However, five of six infants with paucity of intrahepatic bile ducts, two of six infants with cholestasis secondary to total parenteral nutrition, and one infant with cholangiolitis did not show evidence of gastrointestinal excretion. The mean birth weight, mean gestational age, and mean weight at study were significantly greater (P less than 0.005) for infants with biliary atresia without excretion than for infants with intrahepatic cholestasis without excretion. The mean direct bilirubin concentration was 6.0 mg/dL for both infants with biliary atresia and infants with intrahepatic cholestasis without excretion;

however, infants with excretion had a significantly lower (P less than 0.02) mean direct bilirubin value of 3.4 mg/dL. Excretion was noted in four infants with total bilirubin values greater than 10.0 mg/dL. The absence of gut excretion on the first DISIDA study was 100% sensitive but only 43% specific for biliary atresia. In infants without gut excretion of DISIDA, birth weight greater than 2200 g was 100% sensitive and 92% specific for biliary atresia. We conclude that DISIDA scanning, together with clinical data, is useful in differentiating extrahepatic from intrahepatic cholestasis. The absence of gut excretion on the first DISIDA study does not necessarily indicate extrahepatic obstruction; the study should be repeated if the diagnosis is not clear.

Vahid Reza Dabbagh Kakhki et al (2007) described Sincalide, in conjunction with cholescintigraphy, is necessary for the diagnosis of chronic acalculous cholecystitis. However sincalide is not widely available. This study investigates the use of a commercially available formula as an inexpensive alternative to sincalide, containing a sufficient . The aims of their study was to known amount of fat to cause gallbladder contraction, and to determine normal gallbladder ejection fraction (GBEF) values. The data was collected by studied 36 patients aged 51.7±10.9 years with body mass index 26.7± 5.2 who were referred for 99mTc-sestamibi myocardial perfusion imaging. They did not have any abdominal symptoms, or history of abdominal disease and were not taking any medication known to affect the biliary tract. All were prescreened with a hepatobiliary ultrasonography to exclude any abnormality. After 6 hours fasting, 20 mCi of 99mTc-sestamibi was injected intravenously at rest and 90 minutes later the subjects ingested a test meal (10 g fat). GBEF was calculated at 30 and 60 minutes after fatty meal ingestion. The results showed that GBEF at 30 minutes and at 60 minutes after fatty meal ingestion were 69.54±21.04% and 84.26±11.41%, respectively. GBEF did not differ significantly between men and women. There was no statistically significant correlation between BMI and GBEF. No significant difference was noticed in GBEF between obese,

overweight and normal weight patient groups. In Conclusion Lower limit of normal GBEF values was 27.46% at 30 min and 61.44% at 60 min using a standard fatty meal. It is possible to report the results of a GBEF measurement after fatty meal in terms of the percentile rank, compared with subjects without biliary disease.

Jordy J. S et al (2012) described a systematic review and Meta-analysis of DiagnosticPerformance of imaging in acute cholecystitis The aim of their study was To update previously summarized estimates of diagnostic accuracy for acute cholecystitis and to obtain summary estimates for more recently introduced modalities. The data was collected by using asystematic search was performed in MEDLINE, EMBASE, Cochrane Library for5859 patients , and CINAHL databases up to March 2011 to identify studies about evaluation of imaging modalities in patients who were suspected of having acute cholecystitis. Inclusion criteria were explicit criteria for a positive test result, surgery and/or follow-up as the reference standard, and sufficient data to construct a 2 3 2 table. Studies about evaluation of predominantly acalculous cholecystitis in intensive care unit patients were excluded. Bivariate random-effects modeling was used to obtain summary estimates of sensitivity and specificity. The results showed that fifty-seven studies were included, with evaluation of 5859 patients. Sensitivity of cholescintigraphy (96%; 95% confidence interval [CI]: 94%, 97%) was significantly higher than sensitivity of ultrasonography (US) (81%; 95% CI: 75%, 87%) and magnetic resonance (MR) imaging (85%; 95% CI: 66%, 95%). There were no significant differences in specificity among cholescintigraphy (90%; 95% CI: 86% , 93%), US (83%; 95% CI: 74%, 89%) and MR imaging (81%; 95% CI: 69%, 90%). Only one study about evaluation of computed tomography (CT) met the inclusion criteria; the reported sensitivity was 94% (95% CI: 73%, 99%) at a specificity of 59% (95% CI: 42%, 74%). in conclusionc Cholescintigraphy has the highest diagnostic accuracy of all imaging modalities in detection of acute cholecystitis.The diagnostic accuracy of US

has a substantial margin of error, comparable to that of MR imaging, while CT is still underevaluated.

Sadeghi R et al (2009) described 99mTc sestamibi imaging - can it be a useful substitute for hepatobiliary scintigraphy in infantile jaundice. Hepatobiliary scintigraphy is an integral part in the diagnostic work-up of the neonatal cholestasis syndrome. However, less than optimal specificity is its major disadvantage. Differentiation between biliary atresia and neonatal hepatitis is nearly impossible in some cases with poor hepatocellular function. 99mTc sestamibi (MIBI) is a cationic lipophilic agent which is a substrate of P-glycoprotein. This glycoprotein is normally expressed in biliary canalicular surfaces of hepatocytes. This property provides a hepatic excretory mechanism which is different from bilirubin excretion. The aim of their study was to evaluated the value of 99mTc MIBI in differential diagnosis of neonatal cholestasis. The data was collected by using 20 infants with a mean age of 2.41 months (range, 0.1-5 months) were included in the study. Ten infants turned out to have extrahepatic biliary atresia and the other ten had neonatal hepatitis. Hepatobiliary (with 99mTc BrIDA) and 99mTc MIBI scintigraphy were performed for all the patients. The result showed that 99mTc MIBI scintigraphy has shown bowel activity in all patients, including the patients with biliary atresia. Hepatobiliary scintigraphy revealed bowel activity only in five patients with neonatal hepatitis. In conclusion bowel visualization with 99mTc MIBI may be seen in patients with biliary atresia and 99mTc MIBI has limited value in differential diagnosis of neonatal cholestasis.

D. K. Singh et al (2014) described Evaluation of diagnostic efficacy of hepatobiliary scintigraphy as a diagnostic procedure in pediatric practice with special reference to cholestatic jaundice. The aim of their study was to assess the diagnostic efficacy of hepatobiliary scintigraphy (Tc99 mebrofenin) in case of cholestatic jaundice in pediatric practice. The data was collected by using 45 cases from 0-6 yrs. of age. Out of 45 pt 20 pt excluded from study Hepatobiliary Scintigraphy (Tc99m Mebrofinin) was performed in 25 cases. Injection of Tc99m mebrofinin (1-2 mCi) IV was given to each subject. Dynamic hepatic scan was done upto initial 1 hour study and additional delayed images were taken at 4 & 24 hrs only in case of non-visualization of tracer in the intestine after initial 1 hr. study. The results showed that hepatobiliary scintigraphy was 100% sensitive, 93.73% specific, 80% positive predictive values, 100% negative predictive value, 6.23% false positive result and virtually no false negative result for biliary atresia. In conclusion: It is concluded that Tc99m mebrofenin hepatobiliary scintigraphy has proven to be reliable noninvasive imaging modality in evaluating cholestatic jaundice in pediatric practice as it carries a high sensitive & specific value, good positive & no negative predictive value, few false positive & virtually no false negative results.

Seyed Mohsen Dehghani et al (2006) described Comparison of different diagnostic methods in infants with Cholestasis. The aim of their study was to evaluate different methods in differentiating idiopathic neonatal hepatitis from biliary atresia.The data was collected by using sixty-five infants with cholestatic jaundice and final diagnosis of idiopathic neonatal hepatitis and biliary atresia were studied prospectively from September 2003 to March 2006. A thorough history and physical examination were undertaken and the liver enzymes were examined. All cases underwent abdominal ultrasonography, hepatobiliary scintigraphy, and percutaneous liver biopsy. The accuracy, sensitivity, specificity and predictive values of these various methods were compared.The result showed that there were 34 girls and 31 boys, among them 46 subjects had idiopathic neonatal hepatitis (age, 61 ± 17 d) and

19 had biliary atresia (age, 64 ± 18 d). The mean age at onset of jaundice was significantly lower in cases of biliary atresia when compared to idiopathic neonatal hepatitis cases (9 ± 13 d *vs* 20 ± 21 d; *P* = 0.032). The diagnostic accuracy of different methods was as follows: liver biopsy, 96.9%; clinical evaluation, 70.8%; ultrasonography, 69.2%; hepatobiliary scintigraphy, 58.5%; and liver enzymes, 50.8%.In conclusion Our results indicate that clinical evaluation by an experienced pediatric hepatologist and a biopsy of the liver are considered as the most reliable methods to differentiate idiopathic neonatal hepatitis and biliary atresia.

Vahid Reza et al (2007)described normal values of gallbladder ejection fraction using 99mtc-sestamibi scintigraphy after a fatty meal formula. Sincalide, in conjunction with cholescintigraphy, is necessary for the diagnosis of chronic acalculous cholecystitis. However sincalide is not widely available. This study investigates the use of a commercially available formula as an inexpensive alternative. The aims of their study were to sincalide, containing a sufficient and known amount of fat to cause gallbladder contraction, and to determine normal gallbladder ejection fraction (GBEF) values. The data was collected by using studied 36 patients aged 51.7±10.9 years with body mass index 26.7± 5.2 who were referred for 99mTc-sestamibi myocardial perfusion imaging. They did not have any abdominal symptoms, or history of abdominal disease and were not taking any medication known to affect the biliary tract. All were prescreened with a hepatobiliary ultrasonography to exclude any abnormality. After 6 hours fasting, 20 mCi of 99mTc-sestamibi was injected intravenously at rest and 90 minutes later the subjects ingested a test meal (10 g fat). GBEF was calculated at 30 and 60 minutes after fatty meal ingestion. The result showed that GBEF at 30 minutes and at 60 minutes after fatty meal ingestion were 69.54±21.04% and 84.26±11.41%, respectively. GBEF did not differ significantly between men and women. There was no statistically significant correlation between BMI and GBEF. No significant difference was noticed in GBEF between obese, overweight and normal weight

patient groups. In conclusion. Lower limit of normal GBEF values was 27.46% at 30 min and 61.44% at 60 min using a standard fatty meal. It is possible to report the results of a GBEF measurement after fatty meal in terms of the percentile rank, compared with subjects without biliary disease.

Kianifar et al (2013) described Accuracy of hepatobiliary scintigraphy for differentiation of neonatal hepatitis from biliary atresia: systematic review and meta-analysis of the literature. Hepatobiliary scintigraphy is an important diagnostic modality for work-up of neonatal cholestasis. The aim of their study was to evaluate the literature regarding the accuracy of hepatobiliary scintigraphy in differentiating biliary atresia from non-biliary atresia causes of cholestasis (collectively called neonatal hepatitis). The data was collected by using medline, SCOPUS and google Scholar. Only studies using Tc-99 m-labeled immunodiacetic acid (IDA) derivatives were included. Overall, 81 studies were included in the meta-analysis. Pooled sensitivity and specificity were 98.7% (range 98.1–99.2%) and 70.4% (range 68.5–72.2%), respectively. The result showed that the factors that increased specificity included the use of radiotracers with high hepatic extraction, administration of hepatic-inducing drugs (such as phenobarbital), use of a calculated dose/kg and administration of a booster dose in cases of non-excretion of the tracer in the bowel. SPECT imaging and duodenal fluid sampling also had high specificity; however, they need further validation because of the low number of studies. Semiquantitative imaging methods do not seem to have any incremental value. In conclusion that hepatobiliary scintigraphy using IDA derivatives can be very useful for diagnostic work-up of neonatal cholestasis. To improve the specificity, several measures can be followed regarding type and dose of the radiotracer and imaging protocols. Non-imaging methods seem to be promising and warrant further validation.

Chapter three
Methodology

The researcher following the methodology of experimental and practical studies over specific 135 patients suffering from different types of hepatobiliary diseases referring from different clinics to nuclear medicine department to characterization of hepatobiliarysystem function.

All patients who came to the nuclear medicine department to do radionuclide HIDA scan requested by physician for follow up.

3.1Instrument of data collocation

Gamma camera (dual head SPECT)

Type digital

ADAC leberatryies

System ,forte,js, AZ SPECT, ¾

Gauntry ring motion 26%

CE0086

-Radiopharmaceutical

T c^{99m} hydroxy iminodiacetic acid (HIDA).

Technetium has six hours physical half life with its 140 kev gamma emission.

3.2 Sample size

Sample selection of the study was non unstable patient. One hundred and thirty five patients (65 females and 70 males) with the average age 5.5 month under went to get Tc99m HIDA Scintigraphy.

3.3 Method of data collocation

Primary data were collected patients files and interview through question.

Heapatopeliery Scintigraphy with Tc^{99m} HIDA which were requested by doctor.

3.4 methodologies

3.4.1Patient preparation

When the patients were referred for hepatobiliary Scintigraphy. The patients asked for the medication intake if found (stopped for 24hr before the study, as well as to ensure patient NPO 2–14 hours before exam (usually 4–6 hours, 2 hours for infants). And explain the procedures (usually runs ~1 hour but baseline). After the injection the dynamic study immediately started as follows (2 sec/frame for 60 seconds, then immediate blood pool image for flow study and 60 sec/frame for 60–90 minutes for dynamic Studies).

3.4.2 Procedure

Place the patient in supine position, camera anterior (or left anterior oblique), liver in upper left quadrant of field of view (FOV). Position liver in middle FOV if taking immediate heart shadow image, and then move camera to position liver in upper left quadrant of view for remaining images. ROIs can be drawn around heart and heart/liver to ascertain radiotracer clearance from blood pool.

Then every 5 minutes up to 60 minutes. Some take the time in seconds from the 5- or 10-minute view for the rest of the views in the study, giving a better visualization of the radiotracer washout from the liver. If patient can hold still for 60 minutes. Stop dynamic at 30 to 45 minutes if gallbladder and bowel present. Acquire to 90 minutes

if not. Acquire a right lateral (RLAT) static if gallbladder presents. Other useful images may be taken from obliques, laterals, posterior or using pinhole collimators and magnified views for children.

3.5 Variable of data collocation

The data would be taken practically and from reports of the patient.

Social background about patient (age, gender, residence, tribe)weight.

Disease background (symptoms and signs, and type of disease)and the (counts Vs time), to Characterization of hepatobiliary diseases.

3.6 Method of data analysis

Data was entered and analyzed by using Microsoft Excel 2007 and, statistical professional for social science program (spss)

3.7 Study area

The study was done inNuclear Medicine department in Royal care center of Khartoum.

Chapter four

Results

This chapter presents the result which consisted of tables and figures. The table showed distribution age, weight of patient. The figure which showed scatter plot shows the values for count and time for 99mTc–*mebrofenin* obtained in the hepatobiliary studies.

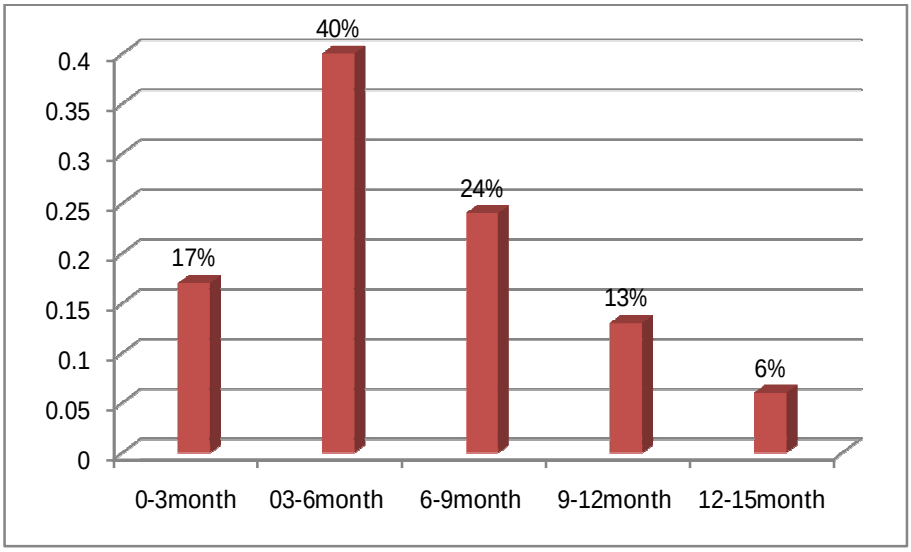

Figure 4.1: shows the frequency and percentage of the sample distributed based on age.

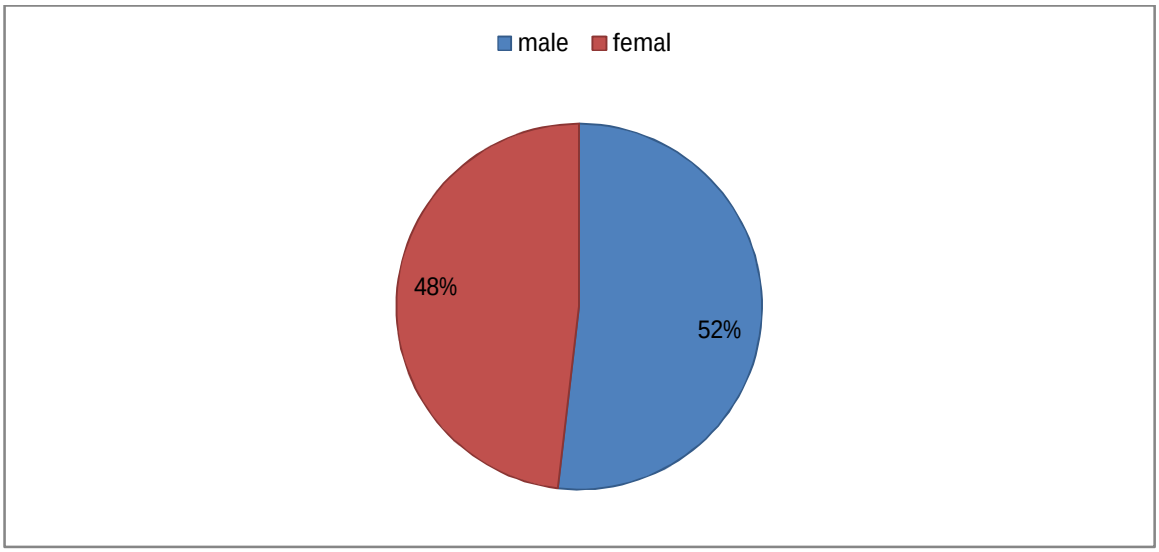

Figure 4.2: show the distribution of gender

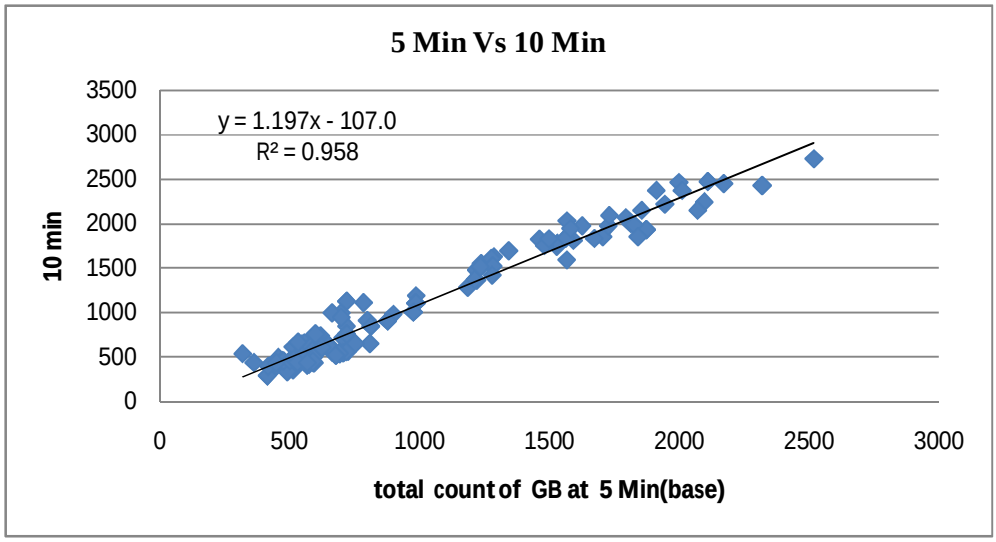

Figure 4.3: time activity curve at time 5 Min base time Vs 10 Min

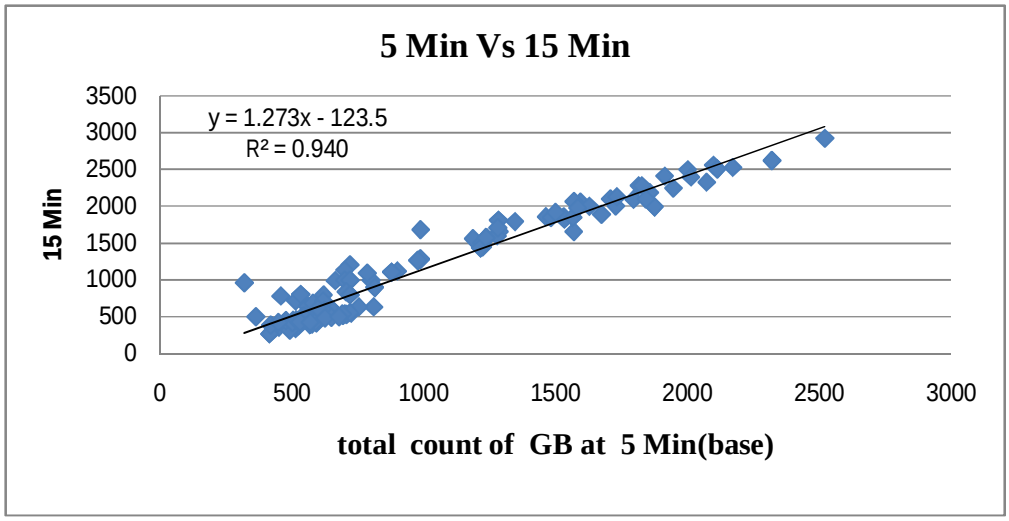

Figure 4.4: time activity curve at time 5 Min Vs 15 Min

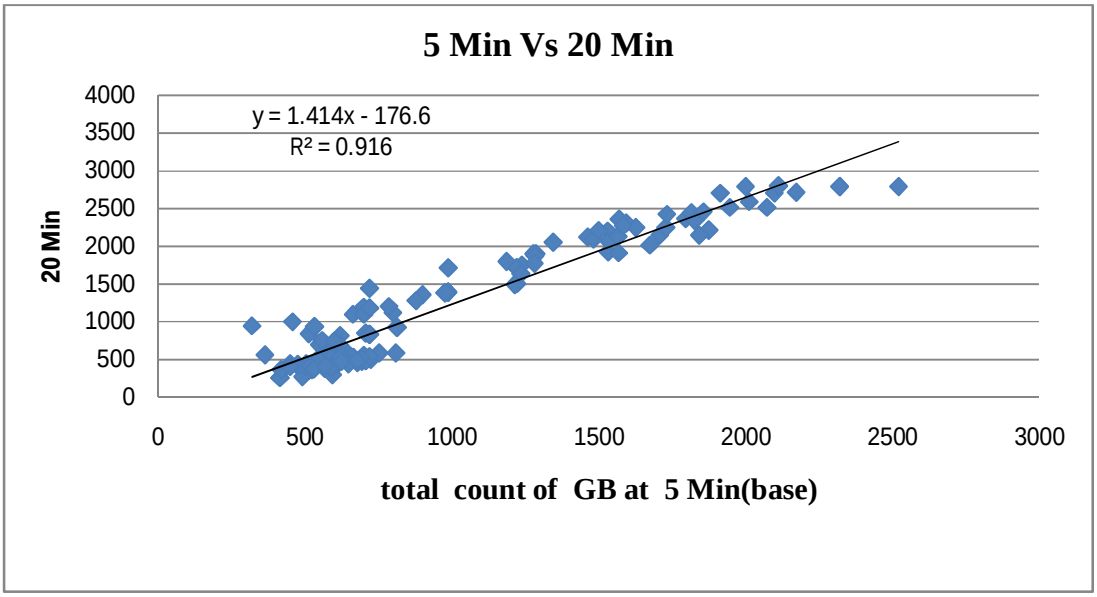

Figure 4.5: time activity curve at time 5 Min Vs 20 Min

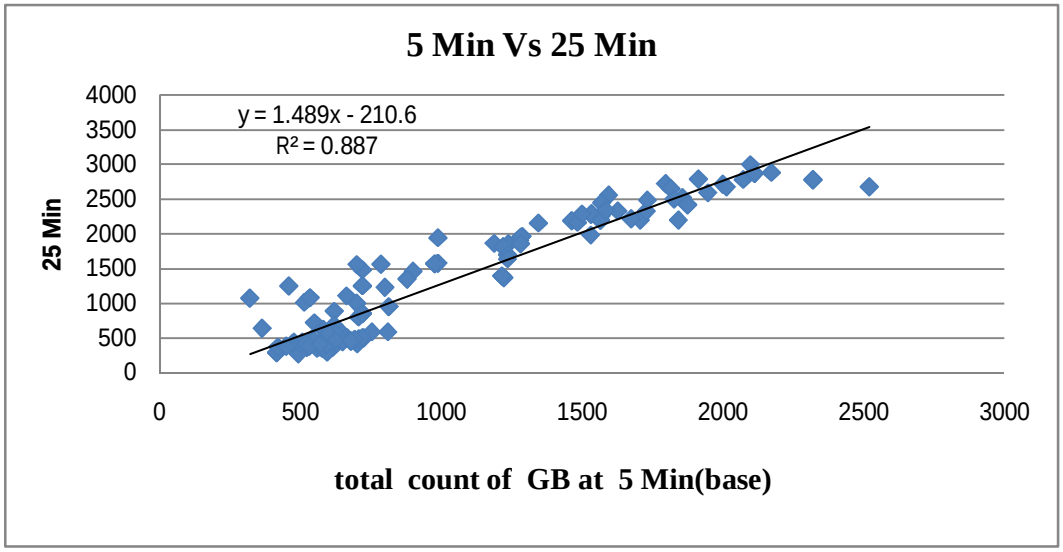

Figure 4.6: time activity curve at time 5 Min Vs 25 Min

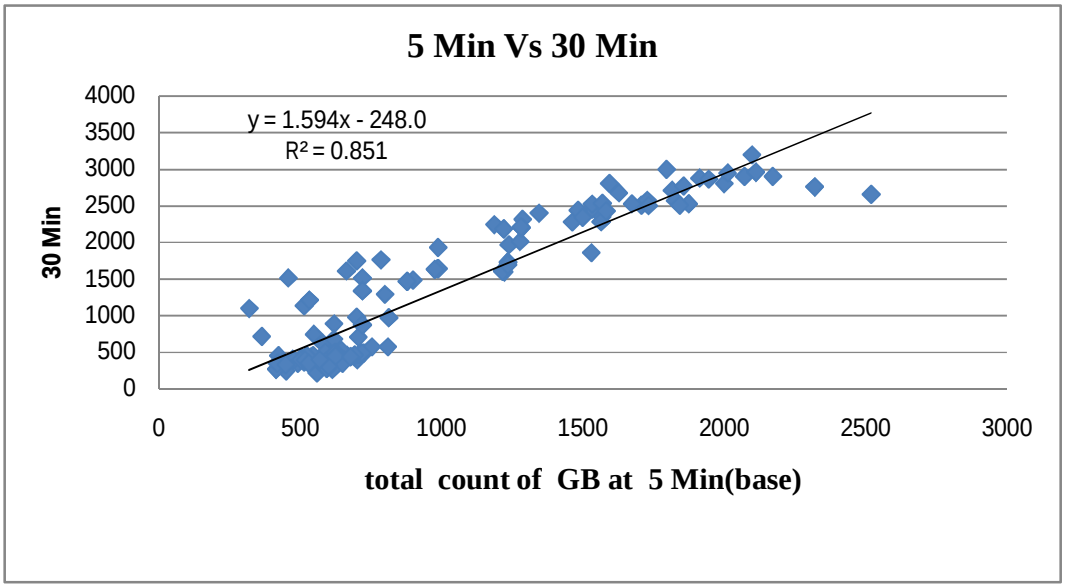

Figure 4.7: time activity curve at time 5 Min Vs 30 Min

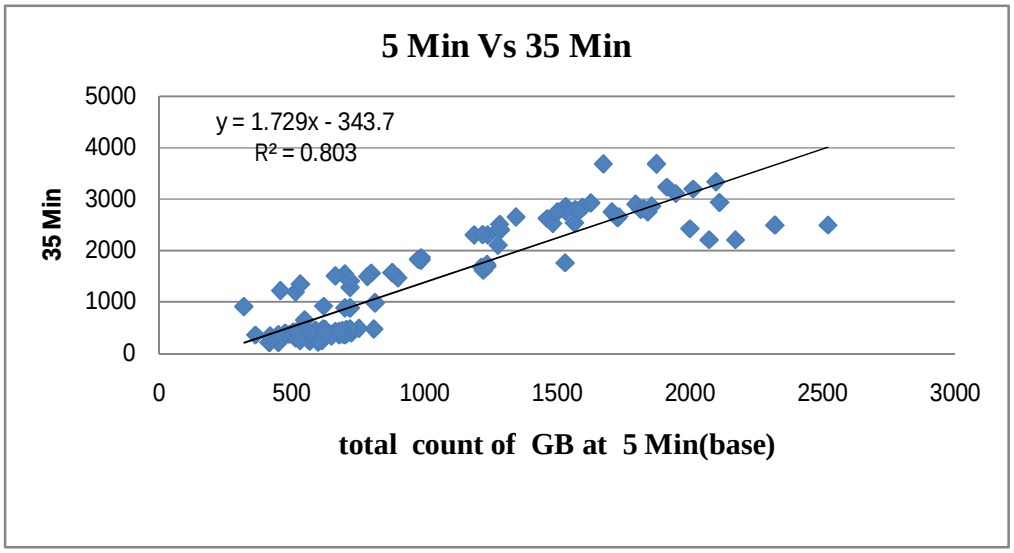

Figure 4.8: time activity curve at time 5 Min Vs 35 Min

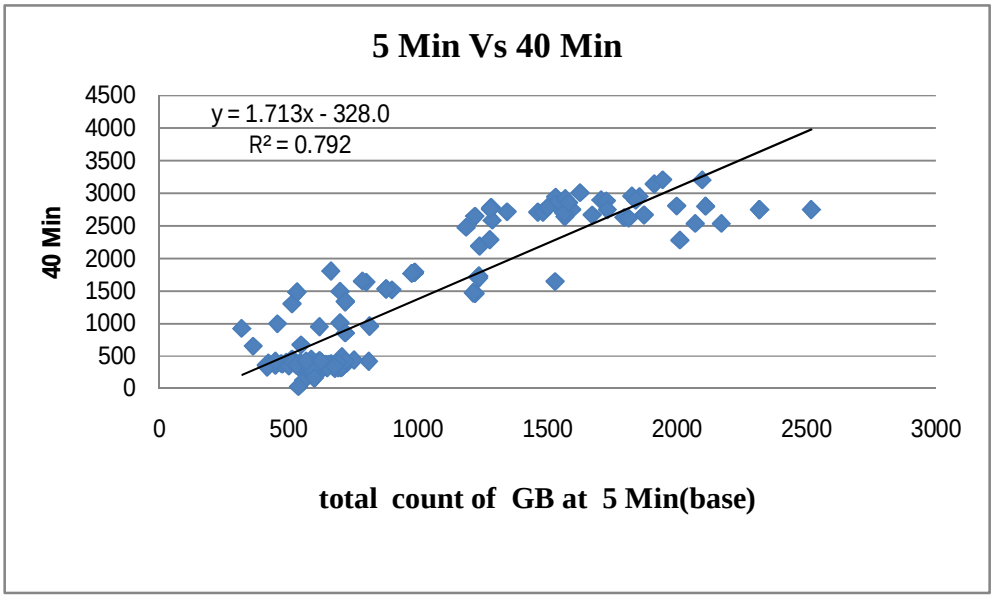

Figure 4.9: time activity curve at time 5 Min Vs 40 Min

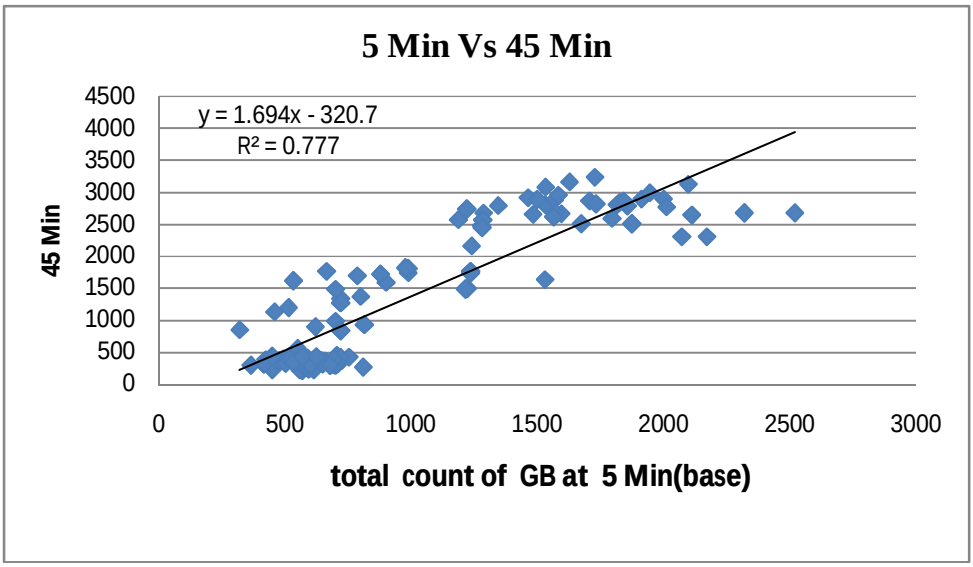

Figure 4.10: time activity curve at time 5 Min Vs 45 Min

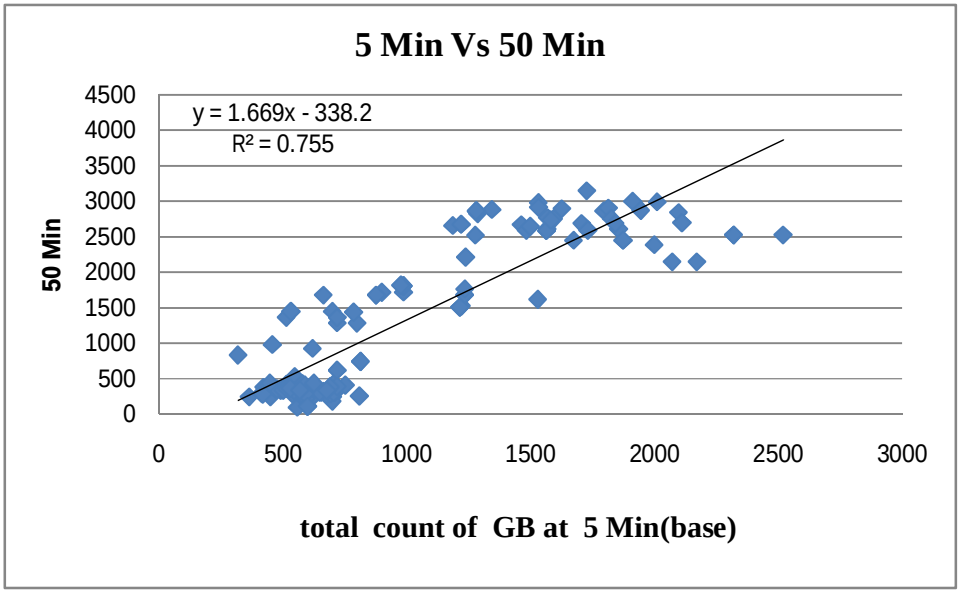

Figure 4.11: time activity curve at time 5 Min Vs 50 Min

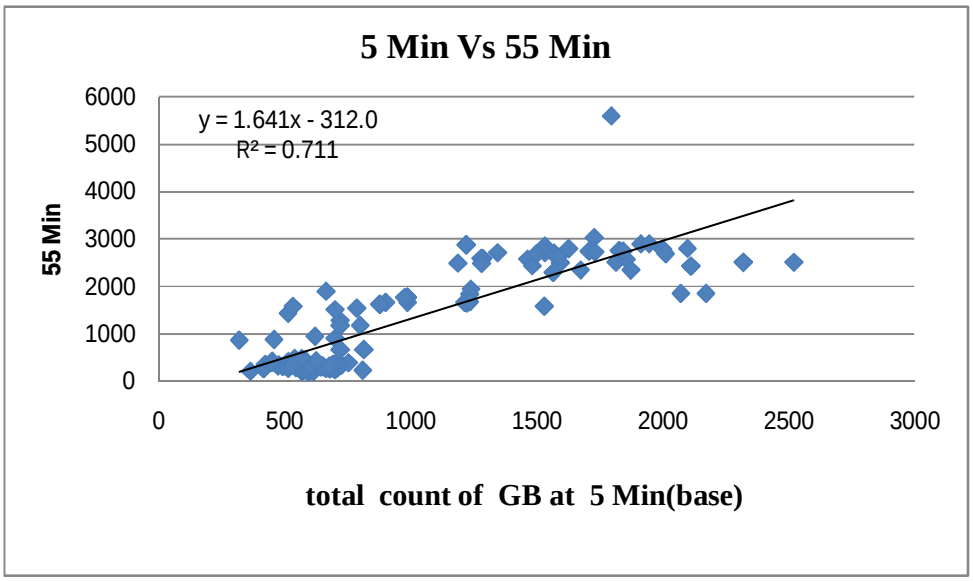

Figure 4.12: time activity curve at time 5 Min Vs 55 Min

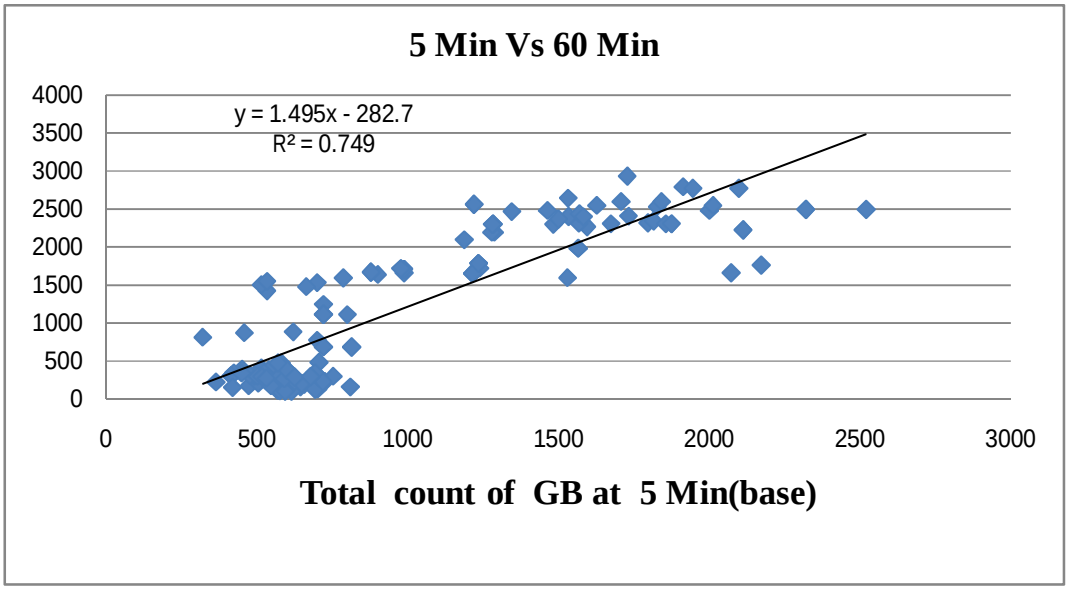

Figure 4.13: time activity curve at time 5 Min Vs 60 Min

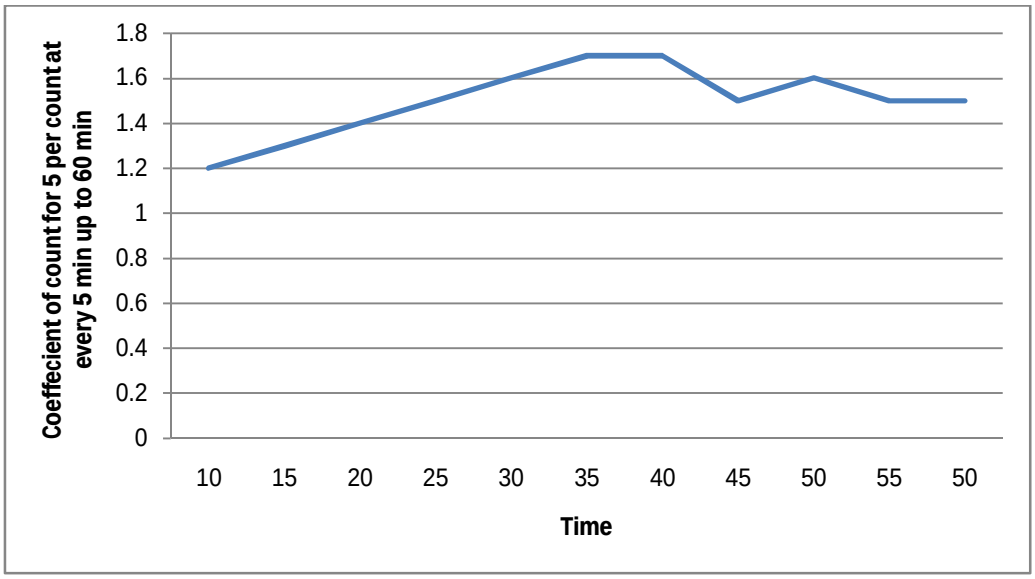

Figure 4.14: show Coefficient of count for 5 per count at every 5 min up to 60 min

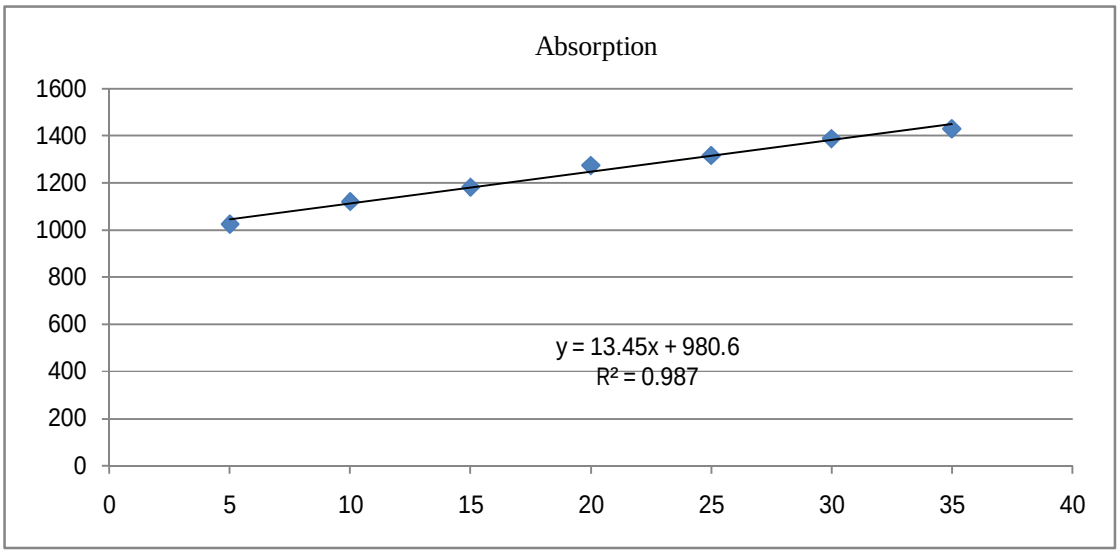

Figure 4.15: show the absorption of radiopharmaceutical (Tc^{99m}HIDA)

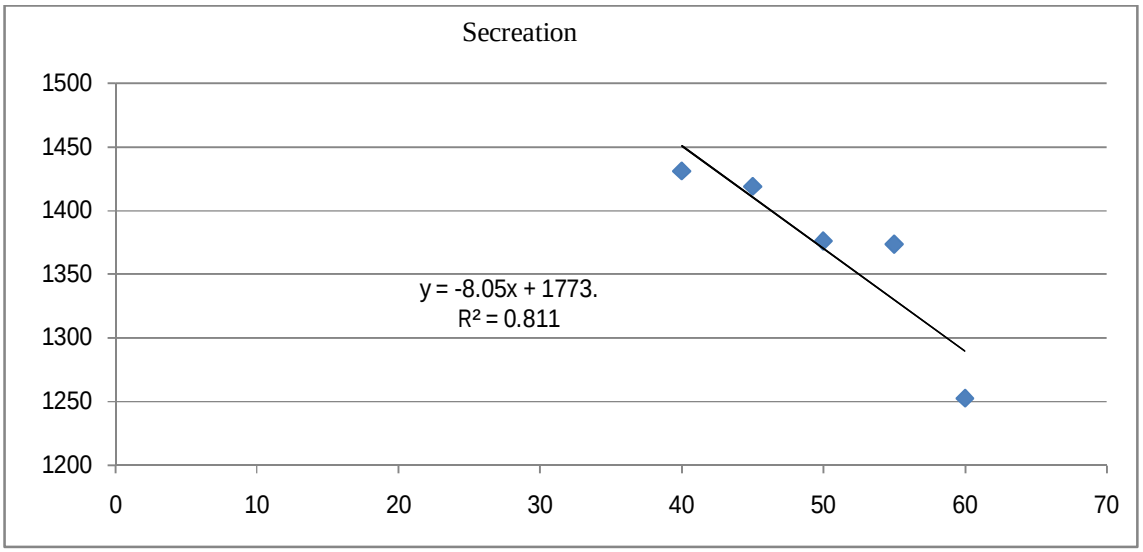

Figure 4.16: show the secretion of radiopharmaceutical (Tc^{99m} HIDA)

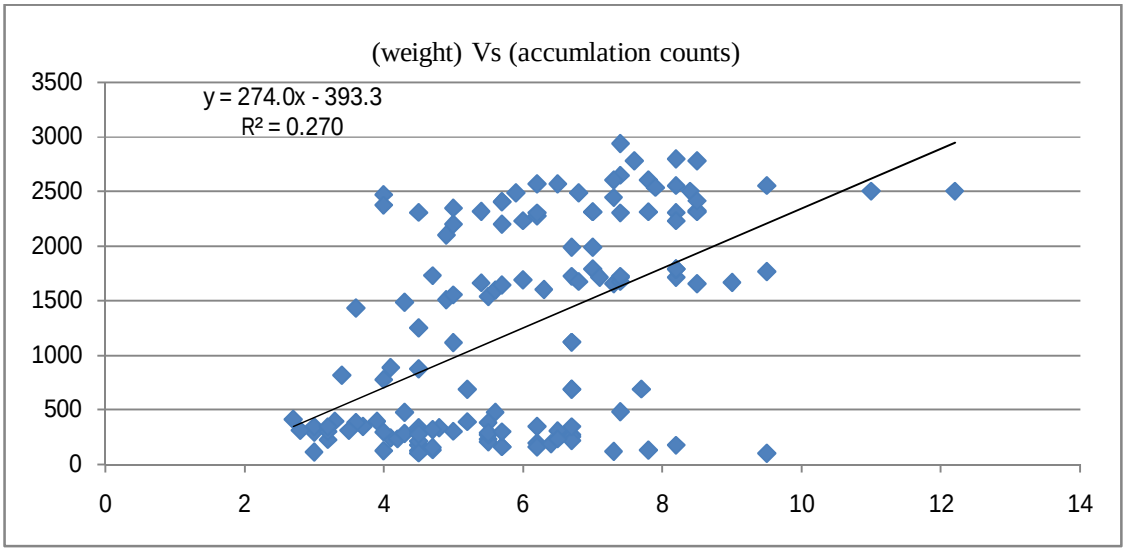

Figure 4.17: show the weight Vs accumulation counts

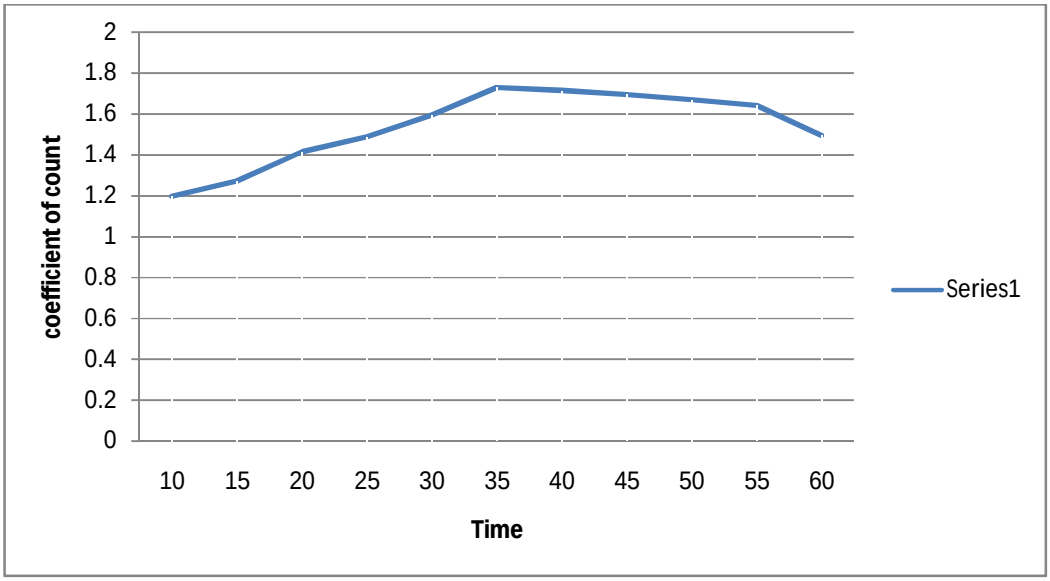

Figure 4.18: show Coefficient of count Vstime every 5 min up to 60 min

Chapter five
Discussion andRecommendation

Assessment of the hepatobiliary system by nuclear medicine techniques in the infant < 12 month of age is usually indicated to help determine the etiology of jaundice. The majority of cases occur in children in the first 3 mo of life. This article primarily addresses the use of hepatobiliary scintigraphy in the neonatal period, but it also identifies other conditions that can occur in the first 12 mo of life. Hyperbilirubinemia in the neonatal period is common, and, in the majority of cases, is due to benign physiological jaundice, a self-limiting condition. Persistent jaundice beyond 2 wk of age in full-term infants and 3 wk in preterm babies is not physio logical, however, and evaluation of these patients must be undertaken (1-3).

5-1 Discussion

This study carried out to Characterization of hepatobiliary scintigraphyusing quantification analysis for infant patient. The study sample consisted of one hundred and thirty five patients patients (70male,65 female) their age ranged from 1to 14 month , (Figure 4-). The weight of the patient ranged between 2.5-12.2 Kg which represents normal body parameter distributions .

Significant differences were seen between counts and time in comparison of the initial count started in 5 min and the counts 10 min. The count from 5 mint to 10 mint,5mint to 15 ,5mint 20 mint ,5mint to 25 and 5mint to 30 mint increase by 1.2 count,1.3 count ,1.4 count ,1.5. count 1.6 count respectively (Figure 4.3 Figure 4.4, Figure 4.5 ,Figure 4.6 and Figure 4.7),but they are see stability of the count in 35 mint ,40, and 45mint . figure 4.8 ,figure 4.9and figure 4.10).

Significant differences were seen between counts and time in comparison of the initial count started in 5 min and the counts 50 min. The count from 5 mint to 50 mint decrease by 1.6 count (Figure 4.11 and 4.12)

The Significant differences also noticed between counts and time in comparison of the initial count started in 5 min and the counts 55 min and 60mint . The count from 5 mint to 55 mint and 60 decrease by 1.6 count and 1.5 count respectively (Figure 4.13 and figure 4.14).

As we can see in (Figure 15)the increases reach a platue at 40 minute from this point up to 60 minute it shows slight decreases but still more the base count at 5 minute.

A number of parameters are calculated from the time activity curves generated from the ROIs placed over the heart (activity in the circulation), liver, hepatic hilum, CBD, and duodenum. The whole liver activity curve analysis initially involved determination of time to the maximal activity (Tmax) and halftime of clearance (T1/2) from Tmax (Gilbert et al. 1987), which is a measure of bile formation and/or impedance to its flow. The absorption of radiotracer uptake started from 5 mint until to 35mint (figure 4.15) .

Figure 4.16. showed the hepatic activity washout, also called percent of radiotracer excreted, can be expressed by a percent clearance from Tmax to a specific time (typically at 30, 45, 60, and 90 min).

As we can see in (Figure 4.17). the absorption of radiopharmaceutical (Tc99m HIDA) From 5mint until 35 mint .shows slight decreases execrations of radiotracer from 35 mint up 60mint but still more the base count at 5 minute.

Finally The majority of cases occur in children in the first 3-6 mo of life (finger 4.1). This article primarily addresses the use of hepatobiliary scintigraphy in the neonatal period, but it also identifies other conditions that can occur in the first 12 mo of life.(Howman-Giles et al et al 1988)

5-2 Conclusion

Hepatobiliary scintigraphy should be used as part of the overall evaluation of neonates and infants with neonatal cholestasis and jaundice.This study carried out to Characterization of hepatobiliary Scintigraphy using Linearequations**.** Thereare various methods for the quantitative analysis of time-radioactivity curves by 99mTc-HIDA liver scintigraphy, ranging from simple methods such as the accumulation rate in the liver and the clearance rate. The study was conducted in Nuclear Medicine department in Royal care center of Khartoum.in the period from 2012 to 2016. The sample of this study consisted of One hundred and thirty five patients (65 females and 70 males) with the average age 5.5 month under went to get Tc99m HIDA Scintigraphy.

5-3 Recommendation

- It is worth recommended to widen the sample size to include different types of hepatobiliry disease.
- single photon emission computed tomography (SPECT) could be acquired with special modifications to provide improved visualization of regional liver function and the biliary tree .
- Further study can be conducted to evaluate the ejection fraction of liver.
- It will be a good application of hepatobiliary scan findings in conjunction with other imaging modalities (e.g., ultrasound).

References

Gilbert SA, Brown PH, Krishnamurthy GT (1987) Quantitative nuclear hepatology. J Nucl Med Technol 15:38-43.

Brown PH, Juni JE, Lieberman DA, Krishnamurthy GT (1988) Hepatocyte versus biliary disease: a distinction by deconvolutional analysis of technetium-99m IDA time-activity curves. J Nucl Med 29:623-630.

Nadel HR (1996) Hepatobiliary scintigraphy in children. Semin Nucl Med 26:25-42.

O'Neill GT, McCreath G (2000) An audit of biliary scintigraphy in a district general hospital (1993-1998) with special reference to the investigation of acalculous gallbladder disease. Nucl Med Commun 21:829-834.

Steiner D, Klett R, Puille M, Doppl W, Bauer R (2003) Diagnosis of focal nodular hyperplasia with hepatobiliary scintig raphy using a modified SPECT technique. Clin Nucl Med 28:136-137.

Stryker J, Siegel A (1997) Abdominal aortic aneurysm visualized with hepatobiliary scintigraphy. Clin Nucl Med **22:**645-646.

Yeh SH, Shih WJ, Liang JC (1973) Intravenous radionuclide hepatography in the differential diagnosis of intrahepatic mass lesions. J Nucl Med 14:565-567.

Los Angeles and California Christiaan Schiepers.2004.DiagnosticNuclearMedicine2nd Revised Edition. *Springer*. chapter 9.135-152.

Graaf D .D, Lienden .K, Dinant .S,1 Roelofs .J, Busch.O, Gouma O. D,1 Bennink O. J,4 and Gulik M.T. (2010). assessment of future remnant liver function using

hepatobiliary scintigraphy in patients undergoing major liver resection. *Springer*. 14(2): 369–378.

Shah I, Bhatnagar S, Rangarajan V, Patankar N.(2012). Utility of Tc99m-Mebrofenin hepato-biliary scintigraphy (HIDA scan) for the diagnosis of biliary atresia. *Pediatric Hepatobiliary Clinic, BJ*.**33(1)**:62-64.

Al Sofayan M.S., Ibrahim A., A. Helmy, M.I. Al Saghier, M.I and M.M. Abozied (2009). Nuclear Imaging of the liver: is there a diagnostic role of HIDA in Posttransplantation. *Elsevier*.**41**:201 -207.

Gerbail T. K and Shakuntala. (2003) Pathophysiology of Acute Critical Obstruction of the Common Bile duct: Role of Quantitative Cholescintigraphy and Ultrasound in Early detection and patient management.*Indian Journal of Nuclear Medicine.***18:**66-71.

Bennink J. R., Dinant S., Erdogan D., Heijnen B.,Straatsburg, I. H. ; Arlene K. , ; and Thomas M. 2003. Preoperative assessment of postoperative remnant liver function using hepatobiliary scintigraphy.*he journal of nuclear medicine JOURNAL .45:965-971.*

Onodera Y., TakahashiK,Togashi T., Sugai.Y, Tamaki D., and Miyasaka K..2003. Clinical assessment of hepatic functional reserve using 99mTc DTPA galactosyl human serum albumin SPECT to prognosticate chronic hepatic diseases validation of the use of SPECT and a new indicator. *Annals of nuclear medicine.***7 (3):** 181–188.

Seyed Mohsen Dehghani,, Neda Efazati,1 Iraj Shahramian, Mahmood Haghighat,1 andMohammad Hadi Imanieh. 2015. Evaluation of cholestasis in Iranian infants less than three months of age.*Gastroenterol Hepatol Bed Bench*. 8(1): 42–48.

Yukio SUGAI, Akio KOMATANI, Takaaki HOSOYA and Kazue TAKAHASHI. (2006). Comparisons of the time-activity curves of the cardiac blood pool and liver uptake by 99mTc-GSA dynamic SPECT and measured 99mTc-GSA blood concentrations.*Annals of Nuclear Medicine*. **20**: 295–301.

Cecilia Diana E. Pîglesan1, Mircea N. Dragoteanu,IoanaGrigorescu and Constantin Cosma (2011) The non-conventional use of 99mTc-Tetrofosmine for dynamic hepatobiliary scintigraphy. *Nuclear Medicine Review* 14**, 2**: 79–84.

Ira Shah,1 SushmitaBhatnagar, 1 VenkateshRangarajanand NikhilPatankar.(2012). Utility of Tc99m-Mebrofenin hepato-biliary scintigraphy (HIDA scan) for the diagnosis of biliary atresia. *Tropical Gastroenterology* **33(1):**62–64.

Roelof J. Bennink, MD1; Sander Dinant, MD2; Deha Erdogan2; Bob H. Heijnen, MD, PhD2;

Irene H. Straatsburg, PhD2; Arlene K. van Vliet, PhD2; and Thomas M. van Gulik, MD, PhD2.(2015) . Preoperative Assessment of Postoperative Remnant Liver Function Using Hepatobiliary Scintigraphy.*The Journal Of Nuclear Medicine.* 45:965-971.

K. Riyad, C.R. Chalmers, A. Aldouri, S. Fraser, K. Menon, P.J. Robinson, and G.J. Toogood (2007). The role of technetiumlabelledhepatoiminodiacetic acid (HIDA) scan in the management of biliary pain .*Oxford*. ; 9(3): 219–224.

Wilmar de Graaf1, Krijn P. van Lienden2, Thomas M. van Gulik1, and Roelof J. Bennink3(2010)99mTc-Mebrofenin Hepatobiliary Scintigraphy with SPECT for the Assessment of Hepatic Function and Liver FunctionalVolume Before Partial Hepatectomy .*The journal of nuclear medicine 51(2):229-236*

Col SS Anand, Lt Col RK Handa, Mr Jogender Singh and Lt Col I Sinha(2006) Hepato-biliary Scintigraphy in diagnosis of Biliary Atresia. *MJAFI*, 62 : 20-21.

Sevilla, Ana MD, Saleh, Hamda , Trpezanovski, Concannon, Rebecca MB BS*; Williams, Katrina David and Uren . 2007. Hepatobiliary Scintigraphy With SPECT in Infancy.*Lippincott Williams & Wilkins* .**32 :** 16-23

Wilmar de Graaf, Krijn P. van Lienden.Thomas M. van Gulik andRoelof J. Bennink **.2010.** ^{99m}Tc-Mebrofenin Hepatobiliary Scintigraphy with SPECT for the Assessment of Hepatic Function and Liver Functional Volume Before Partial Hepatectomy.*The journal of nuclear medicine.* **51**:229–236.

Robert Matthews, Mera Goodman, PryankaRelan, ElhamSafaie, and DinkoFranceschi.2013. Tc-99m Mebrofenin Hepatobiliary Scan in Obstructive Hepatobiliary Disease: Determining Causes with Early and Late Delayed Imaging.*World J Nucl Med*. 12(2): 54–56.

Kevin J. Gaskin, Donna L.M. Waters, Robert Howman-Giles, Merl De Silva, John W. Earl, Hugh C.O. Martin, Alex E. Kan, John M. Brown, and Stuart F.A. Dorne.1988. Liver Disease and Common-Bile-Duct Stenosis in Cystic Fibrosis. *N Engl J Med* , 318:340-346.

Spivak W, Sarkar S, Winter D, Glassman M, Donlon E and Tucker KJ.1987. Diagnostic utility of hepatobiliary scintigraphy with 99mTc-DISIDA in neonatal cholestasis. *J Pediatr*. 110(6):855-61.

Vahid Reza Dabbagh Kakhki1, Seyed Rasoul Zakavi1, Yasmin Davoudi .2007 . Normal values of gallbladder ejection fraction using 99mTc-sestamibi scintigraphy after a fatty meal formula . *J Gastrointestin Liver Dis* .**2:**157-161.

Jordy J. S. Kiewiet, Marjolein M. N. Leeuwenburgh, Shandra Bipat, Patrick M. M. Bossuyt, Jaap Stoker, and Marja A. Boermeester, 2012.a systematic review and Meta-analysis of Diagnostic Performance of imaging in acute cholecystitis. *Radiology*: 264: (3)70-720.

Sadeghi R, Kianifar HR, Kakhki VR, Zakavi SR, Ansari K .2009. 99mTc sestamibi imaging - can it be a useful substitute for hepatobiliary scintigraphy in infantile jaundice.*Nuklearmedizin.* **48(3):**100-103.

D. K. Singh, Rajesh Kumar Yadav, Mukesh Veer Singh, Mamta Singh, D. K. Hazra, Meena Singh. 2014 Evaluation of diagnostic efficacy of hepatobiliary scintigraphy

as a diagnostic procedure in pediatric practice with special reference to cholestatic jaundice..*International Journal of Research in Medical Sciences* .2(4): 1563-1568.

Seyed Mohsen Dehghani, Mahmood Haghighat, Mohammad Hadi Imanieh, and Bita Geramizadeh . 2006. Comparison of different diagnostic methods in infants with Cholestasis..*World J Gastroenterol*. 2006 Sep 28; 12(36): 5893–5896.

Vahid Reza Dabbagh Kakhki1 , Seyed Rasoul Zakavi1 and Yasmin Davoudi.2007. Normal Values of Gallbladder Ejection Fraction Using 99mTc-sestamibi Scintigraphy after a Fatty Meal. *FormulaJ Gastrointestin Liver* Dis 16 (2) 157-161.

Hamid Reza Kianifar, Shahrzad Tehranian, Pardis Shojaei, Zohreh Adinehpoor, Ram in Sadeghi, Vahid Reza Dabbagh Kakhki and Alireza S. Keshtgar . 2013. Accuracy of hepatobiliary scintigraphy for differentiation of neonatal hepatitis from biliary atresia: systematic review and meta-analysis of the literature.. *Pediatric Radiology* .43(8) : 905–919.

Appendix A

Images of hepatobiliary scan (HIDA)

ROYAL CARE INTERNATIONAL HOSPITAL

Nuclear medicine departement

LIVER SCAN WITH TC99-M HIDA

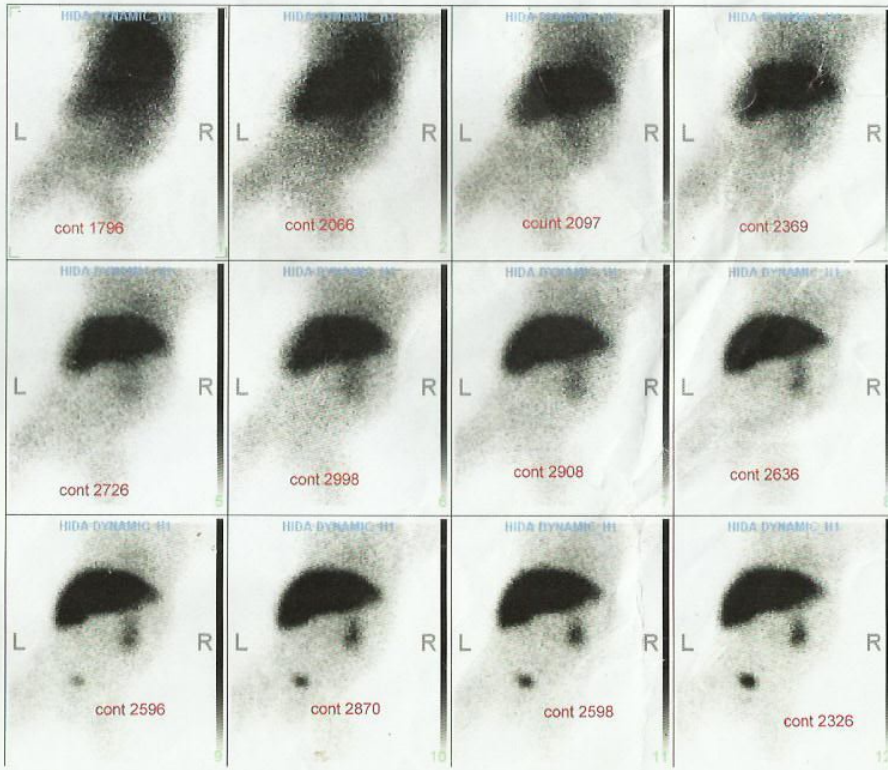

ROYAL CARE INTERNATIONAL HOSPITAL

Nuclear medicine departement

LIVER SCAN WITH TC99-M HIDA

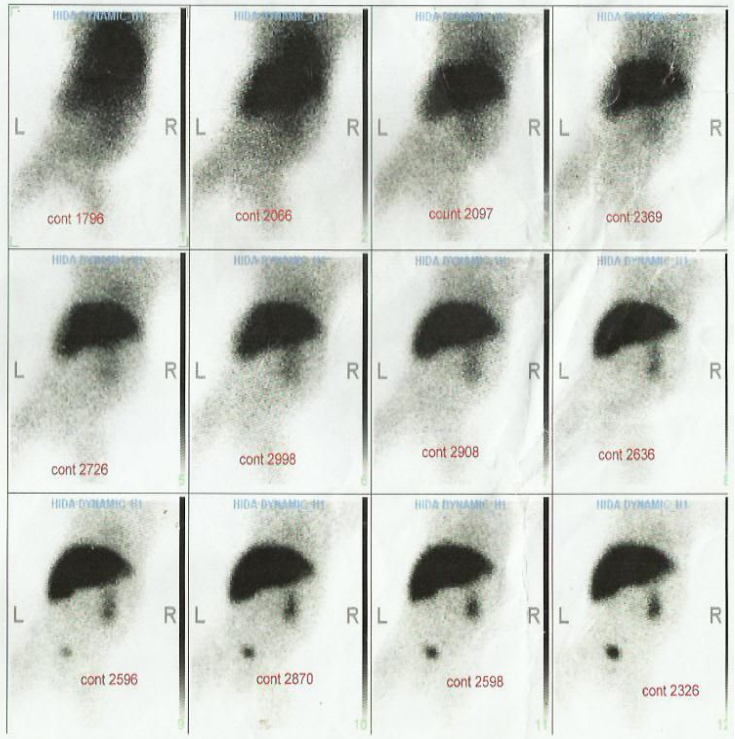

Appendix B

Data sheet

O	Age	Gen0der	weight	Count per min at time											
				5	10	15	20	25	30	35	40	45	50	55	60
1	3m	M	3.9	514	391	375	364	380	372	351	459	415	396	282	400
2	7m	F	5.9	1463	1824	1863	2127	2191	2281	2629	2717	2922	2673	2585	2487
3	2m	M	3.4	320	542	964	953	1071	1100	915	931	855	834	876	819
4	4m	F	4.5	720	851	1211	1450	1483	1519	1289	1351	1342	1290	1289	1252
5	8m	F	6.3	1530	1745	1861	2209	1984	1862	1765	1650	1639	1619	1589	1604
6	11m	F	7.3	1215	1372	1439	1500	1394	1610	1682	1479	1491	1509	1671	1657
7	1m	M	2.7	514	359	342	384	395	387	300	450	433	419	427	416
8	12m	F	7.6	2098	2245	2560	2712	3000	3198	3341	3212	3131	2845	2809	2780
9	14m	M	8.4	2320	2428	2625	2794	2781	2760	2501	2758	2684	2530	2515	2503
10	2m	M	3.7	692	547	540	523	478	462	452	402	394	383	369	350
11	5m	F	5	800	913	1000	1124	1230	1294	1567	1640	1375	1286	1190	1117
12	9m	F	6.7	720	1131	1001	1189	1250	1344	1418	1339	1276	1364	1183	1121
13	10m	F	7	1235	1513	1576	1640	1698	1735	1705	1738	1769	1687	1853	1791
14	6m	F	5.5	700	1000	1136	1201	1560	1749	1552	1500	1487	1453	1518	1539
15	3m	M	4.1	620	741	798	822	886	891	924	957	900	930	959	890
16	3m	M	4.3	664	1000	994	1106	1106	1613	1513	1813	1768	1681	1908	1486
17	4m	F	4.7	701	577	543	566	411	400	362	324	293	250	259	136
18	5m	F	5.4	988	1190	1687	1720	1945	1936	1867	1800	1745	1723	1673	1665
19	5m	F	5.2	814	851	900	934	949	976	989	965	934	747	682	691
20	9m	F	7.1	987	1109	1287	1398	1576	1645	1823	1787	1814	1809	1779	1716
21	8m	F	6.8	2000	2461	2500	2794	2718	2804	2429	2813	2901	2392	2788	2488
22	7m	F	5.6	786	1115	1098	1210	1562	1765	1500	1659	1699	1440	1549	1599
23	3m	M	5.7	900	982	1125	1365	1459	1490	1473	1524	1596	1719	1673	1646
24	3m	M	6	1222	1365	1452	1512	1367	1598	1618	1468	1500	1530	1659	1691
25	2m	M	3.6	533	669	805	941	1078	1214	1350	1486	1623	1451	1587	1433
26	2m	M	4.5	549	650	684	705	719	750	652	678	562	529	350	338
27	5m	F	6.2	1594	1813	2062	2311	2560	2809	2848	2760	2672	2759	2510	2275
No	**Age**	**Gender**	**weight**	**Count per min at time**											
				5	**10**	**15**	**20**	**25**	**30**	**35**	**40**	**45**	**50**	**55**	**60**

28	2m	M	3.6	600	761	614	749	559	319	232	168	309	112	323	385
29	2m	M	4	568	413	396	387	364	259	245	230	219	211	232	127
30	5m	F	5.7	1287	1628	1663	1908	1965	2317	2409	2593	2681	2826	2598	2201
31	5m	M	6.2	1220	1481	1507	1724	1814	2189	2315	2656	2744	2679	2886	2569
32	6m	F	6.7	1565	1840	1855	2134	2197	2287	2541	2708	2620	2589	2302	1990
33	7m	M	7.4	1532	1780	1840	1928	2276	2459	2863	2952	2810	2984	2861	2649
34	8m	F	7.8	1707	1854	2101	2151	2200	2512	2759	2905	2871	2691	2751	2606
35	9m	M	8.2	1913	2374	2413	2707	2791	2881	3238	3150	2901	305	2904	2799
36	12m	M	8.5	1796	2066	2097	2369	2726	2998	2908	2636	2596	2870	5598	2326
37	14m	F	9.5	2012	2373	2402	2596	2676	2951	3199	2287	2778	2994	2694	2554
38	3m	M	5.4	1568	1593	1658	1917	2265	2355	2802	2649	2888	2612	2710	2318
39	3m	M	4.9	1187	1285	1563	1803	1864	2245	2310	2486	2578	2662	2498	2102
40	4m	M	5.7	1533	1778	1829	2074	2292	2526	2763	2847	3088	2917	2725	2409
41	5m	F	6.2	1483	1755	1848	2097	2165	2439	2529	2717	2661	2596	2444	2304
42	3m	M	4.7	1239	1551	1576	1760	1857	1972	2307	2195	2167	2217	1951	1730
43	2.5m	F	4.1	665	556	549	538	501	463	429	391	356	322	284	246
44	7m	F	7.4	1728	1977	2006	2255	2329	2578	2644	2893	3241	3151	3037	2939
45	9m	M	8.2	1627	1975	2004	2253	2333	2681	2930	3018	3170	2898	2803	2554
46	10m	F	8.5	1946	2218	2248	2520	2594	2866	3115	3217	2998	2874	2907	2780
47	8m	M	7.3	1569	2030	2069	2363	2447	2537	2801	2923	2683	2772	2689	24456
48	1m	M	3.2	364	442	504	568	639	721	362	658	300	246	222	230
49	2m	M	4	700	950	1000	1105	1000	980	892	1014	987	186	915	780
50	3m	M	4.5	458	500	786	1007	1247	1518	1226	1000	1134	982	892	878
51	3m	F	3.3	450	400	361	452	386	245	217	363	230	249	436	400
52	4m	F	5.5	725	570	553	511	500	492	405	390	376	368	351	236
53	4m	F	5.7	810	655	638	596	585	577	481	423	268	257	245	165
54	3.5m	F	3	612	589	603	564	526	488	450	412	384	375	337	298
Nom	**Age**	**Gender**	**weight**	**Count per min at time**											
				5	**10**	**15**	**20**	**25**	**30**	**35**	**40**	**45**	**50**	**55**	**60**
55	1.5m	M	3.5	415	293	273	266	284	271	219	361	317	298	283	314
56	2m	M	4.5	569	415	400	397	384	359	345	230	219	211	232	127
57	5m	F	5	1278	1608	1603	1908	1905	2017	2109	2293	2481	2526	2598	2201

58	5m	F	6.5	1220	1481	1507	1724	1814	2189	2315	2656	2744	2679	2886	2569
59	6m	M	7	1565	1840	1855	2134	2197	2287	2541	2708	2620	2589	2302	1990
60	7m	F	7.4	878	908	1109	1285	1348	1472	1576	1535	1726	1681	1634	1676
61	8m	F	7.8	1874	1934	1995	2220	2419	2531	3689	2674	2514	2454	2353	2314
62	9m	M	8.2	987	1109	1287	1398	1576	1645	1823	1787	1814	1809	1779	1716
63	12m	F	9	2072	2151	2331	2519	2785	2903	2213	2544	2310	2149	1860	1668
64	14m	M	12.2	2520	2728	2925	2794	2681	2660	2501	2758	2684	2530	2515	2503
65	6m	F	6.7	720	1131	1001	1189	1250	1344	1418	1339	1276	1364	1183	1121
66	3m	M	4.9	514	616	718	848	1012	1139	1201	1307	1203	1368	1445	1510
67	4m	F	5.7	645	646	623	587	576	529	384	377	369	333	310	165
68	5m	F	6.2	656	624	586	548	496	393	382	374	358	314	305	198
69	3m	M	4.8	559	661	644	761	345	219	289	125	223	99	276	339
70	6m	M	6.7	977	1009	1267	1389	1567	1634	1832	1777	1824	1819	1776	1724
71	7m	F	7.4	987	1109	1287	1398	1576	1645	1823	1787	1814	1809	1779	1716
72	9m	M	8.2	1235	1513	1576	1640	1698	1735	1705	1738	1769	1687	1853	1791
73	10m	M	8.5	1215	1372	1439	1500	1394	1610	1682	1479	1491	1509	1671	1657
74	8m	F	7	1674	1834	1895	2020	2219	2531	3689	2674	2514	2454	2353	2314
75	1m	M	3	423	400	384	363	357	457	313	395	386	381	367	349
76	2m	M	4.5	473	466	432	432	423	409	398	389	352	345	332	178
77	3m	M	5.2	539	519	504	492	479	441	404	35	327	289	496	393
78	3m	M	5.6	580	620	687	589	619	626	387	324	415	434	458	482
79	4m	M	6.5	619	596	719	700	689	682	481	403	325	281	267	311
80	4m	M	6.7	625	619	586	569	558	501	473	381	374	356	349	274
81	6m	F	7.7	720	761	802	839	852	879	890	861	840	622	679	693
No	**Age**	**Gender**	**weight**	**Count per min at time**											
				5	**10**	**15**	**20**	**25**	**30**	**35**	**40**	**45**	**50**	**55**	**60**
82	1.5m	M	3	576	421	404	396	354	345	303	289	264	253	238	115
83	2m	M	4.2	709	554	537	495	486	475	388	338	323	309	301	237
84	5m	F	5	1815	2000	2281	2451	2654	2715	2804	2625	2812	2909	2517	2349
85	5m	M	6.2	592	437	420	412	404	362	275	261	246	237	226	162
86	6m	M	6.7	679	524	507	465	454	446	359	309	294	280	272	258
87	7m	M	7.4	706	720	845	856	800	713	471	492	455	430	396	486

88	8m	F	7.8	693	538	521	479	468	460	373	323	309	294	283	135
89	9m	F	8.2	1283	1525	1813	1877	1957	2204	2514	2789	2570	2866	2590	2308
90	12m	F	9.5	2172	2451	2531	2719	2885	2903	2213	2544	2310	2149	1860	1768
91	14m	F	9.5	614	572	561	511	356	269	255	240	231	220	212	105
92	3m	M	4.5	505	467	458	451	440	431	420	411	388	351	361	213
93	3m	M	4	1345	1697	1795	2059	2157	2402	2656	2725	2797	2887	2717	2473
94	4m	F	6	2112	2473	2509	2803	2871	2961	2939	2810	2651	2701	2437	2232
95	5m	F	6.4	589	578	536	527	513	504	462	455	417	411	256	192
96	3m	F	4.5	1283	1525	1813	1877	1957	2204	2514	2789	2570	2866	2590	2309
97	6m	M	6.7	620	596	587	537	472	488	477	439	415	375	361	220
98	7m	F	7.4	1281	1421	1712	1778	1859	2214	2418	2768	2454	2865	2496	2305
99	9m	F	8.2	546	525	516	505	467	456	447	409	371	333	295	178
100	10m	F	8.5	1856	2150	2189	2463	2523	2772	2871	2959	2790	2613	2581	2314
101	8m	M	7.3	595	440	423	381	372	285	271	256	245	236	228	122
102	1m	M	3.2	753	655	638	596	585	577	490	442	425	411	403	306
103	2m	M	4	1500	1830	1922	2214	2289	2346	2756	2789	2895	2648	2699	2375
104	3m	M	4.5	594	505	463	308	291	280	266	251	240	224	207	107
105	3m	M	4.3	706	551	534	492	481	473	386	336	321	307	299	286
106	4m	F	5.5	649	632	494	452	444	354	341	325	320	311	339	210
107	4m	F	5.7	1583	1944	1983	2277	2341	2431	2773	2861	2960	2741	2629	2405
108	6m	F	6.7	523	400	384	373	357	457	313	395	386	381	367	349
Nom	**Age**	**Gender**	**weight**	**Count per min at time**											
				5	**10**	**15**	**20**	**25**	**30**	**35**	**40**	**45**	**50**	**55**	**60**
109	1.5m	F	2.8	415	293	273	266	284	271	219	361	317	298	283	314
110	2m	M	4.7	419	400	391	373	368	353	342	334	325	287	280	158
111	5m	F	5	533	669	805	941	1078	1214	1350	1486	1623	1451	1587	1555
112	5m	F	5.5	590	455	438	400	392	381	358	314	303	288	256	272
113	6m	M	6.5	719	564	559	548	506	495	488	426	418	394	344	236
114	7m	F	6.8	878	908	1109	1285	1348	1472	1576	1535	1726	1681	1634	1676
115	8m	F	7	1874	1934	1995	2220	2419	2531	3689	2674	2514	2454	2353	2314
116	9m	F	7.9	1827	1988	2282	2343	2501	2576	2821	2966	2851	2761	2761	2537
117	12m	F	8.2	2112	2473	2509	2803	2871	2961	2939	2810	2651	2701	2437	2232

118	14m	M	11	2320	2428	2625	2794	2781	2760	2501	2758	2684	2530	2515	2503
119	3m	M	4.5	492	337	320	278	267	354	376	404	389	339	328	311
120	3m	M	4.7	477	460	452	441	435	399	394	382	371	359	362	320
121	4m	F	5	502	464	426	420	413	402	376	356	325	337	333	305
122	5m	F	6.2	692	547	540	523	478	467	452	402	394	383	369	350
124	3m	M	5.5	600	761	614	749	559	319	232	168	309	112	323	385
125	6m	F	6.7	814	851	900	934	949	976	989	965	934	747	682	691
126	7m	F	7.4	977	1009	1267	1389	1567	1634	1832	1777	1824	1819	1776	1724
127	9m	F	8.2	1235	1515	1576	1640	1640	1698	1735	1705	1738	1769	1687	1791
128	10m	F	8.5	1732	2093	2132	2429	2490	2505	2665	2753	2824	2594	2731	2415
129	8m	F	7.3	1842	1854	2101	2151	2200	2512	2759	2905	2871	2691	2751	2606
130	1m	M	3.2	449	438	429	411	373	334	376	426	438	442	402	348
131	2m	M	4	517	479	460	418	410	399	419	409	399	361	311	300
132	3m	M	4.5	531	443	432	380	377	354	255	364	345	367	349	279
134	3m	M	4.3	569	441	430	422	411	403	414	423	429	338	493	479
135	4m	M	5.5	625	610	487	478	467	453	411	420	428	439	448	293
136	4m	F	5.7	678	523	506	495	453	442	434	347	297	337	335	301
137	6m	M	6.7	720	761	802	839	852	879	890	861	840	622	679	693

Appendix C

Gamma camera

Mode of Operation of the GammaCamera

The image of the distribution of the gamma-ray-emitting radio pharmaceutical is produced in the scintillation crystal by a collimator. The gamma rays, which are not visible to the eye, are converted into flashes of light by the scintillation crystal. This light is, in turn, transformed into electronic signals by an array of photomultiplier tubes (PMT) viewing the rear face of the crystal. After processing, the outputs from the PMTs are converted into three signals, two of which (X and Y) give the spatial location of the

Scintillation while the third (Z) represents the energy deposited in the crystal by the gamma ray. To improve their quality these signals then pass through correction circuits. The Z signal goes to a pulse height analyzer (PHA), which tests whether the energy of the gamma ray is within the range of values expected for the particular radionuclide

being imaged. If the Z signal has an acceptable value, then a signal is sent instructing the display to record that there between gamma ray detected, the position being determined by the X and Y signals. The individual elements of the system will now be considered in more detail.

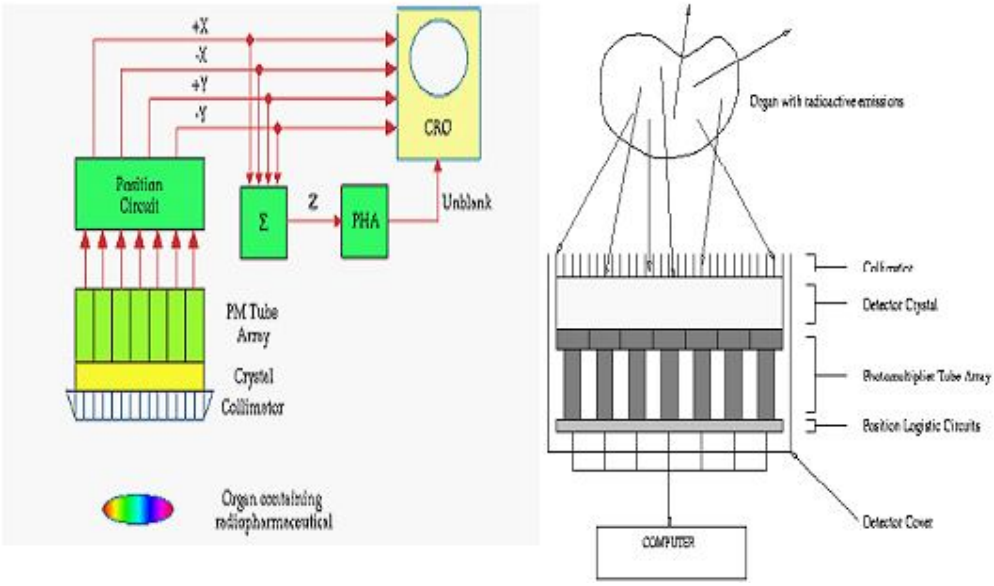

Figure (A-1) showing basic principles of gamma camera and of components of a gamma camera

Collimator

The collimator is a device which is attached to the front of the gamma camera head. It functions something like a lens used in a photographic camera but this analogy is not quite correct because it is rather difficult to focus gamma-rays. Nevertheless in its simplest form it is used to block out all gamma rays which are heading towards the crystal except those which are travelling at right angles to the plane of the crystal.

The collimator simply consists of a large number of small holes drilled in a lead plate. Notice that gamma rays entering at an angle to the crystal get absorbed by the lead and that only those entering along the direction of the holes get through to cause scintillations in the crystal. If the collimator was not in place these obliquely incident gamma-rays would blur the images produced by the gamma camera. In other words the images would not be very clear.

Most gamma cameras have a number of collimators which can be fitted depending on the examination. The basic design of these collimators is the same except that they vary in terms of the diameter of each hole, the depth of each hole and the thickness of lead between each hole (commonly called the septum thickness). The choice of a specific collimator is dependent on the amount of radiation absorption that occurs (which influences the sensitivity of the gamma camera), and the clarity of images (that is the spatial resolution) it produces. Unfortunately these two factors are inversely related in that the use of a collimator which produces images of good spatial resolution generally implies that the instrument is not very sensitive to radiation.

Other collimator designs beside the parallel hole type are also in use. For example a diverging hole collimator produces a minified image and converging hole and pin-hole collimators produce a magnified image. The pin-hole collimator is illustrated in the following figure:

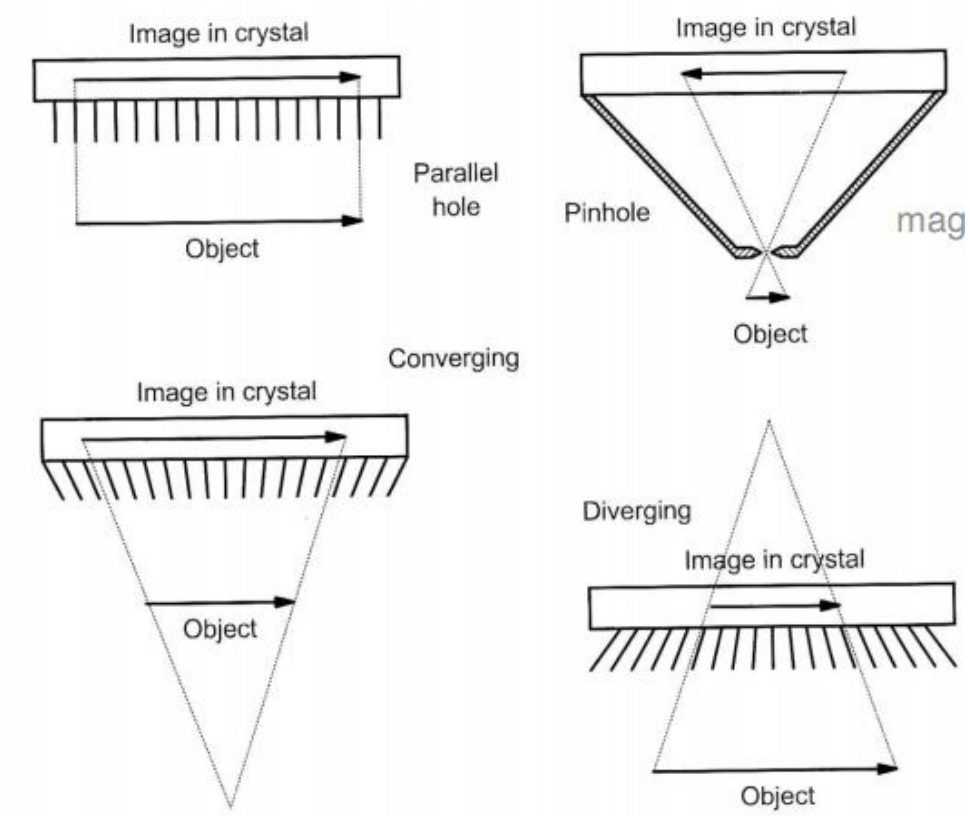

Figure (A-2)shows Different types of collimator. the field of view of the collimator and the image in crystal.

The Scintillation Crystal

Most common is to use a thin and large circular crystal made of sodium iodide (NaI), activated with a trace of thallium (Tl) as scintillation. It has a diameter of 30-50 cm and its thickness is a trade-off between intrinsic resolution (the spatial resolution of the system without collimator) and detection efficiency of the incident photons. Due to the fact that most gamma cameras are designed for imaging 99mTc-labeled pharmaceuticals with 140 kev low-energy γ photon emissions, a crystal thickness of 9-12 mm provides the best compromise between resolution and efficiency.

Light Guides

It is usually necessary to provide a light guide to interface the scintillation crystal to the photomultipliers. This light guides are made of transparent plastic with a Refractive index close to 1.85, the refractive index of NaI(Tl), and they are carefully shaped to match the shape of the photomultiplier entrance window . The light guide helps to minimize the light losses in the transfer of light from the scintillation crystal to the photomultiplier. It will also minimize the variation of light collection efficiency across the face of the crystal.

Photomultiplier Tube (PMT)

A scintillator coupled to a photomultiplier tube (PMT).The overall device is typically cylindrical in shape and it consists of a photocathode, a focusing grid, an array of dynodes and an anode housed in an evacuated glass tube as shown in Fig().

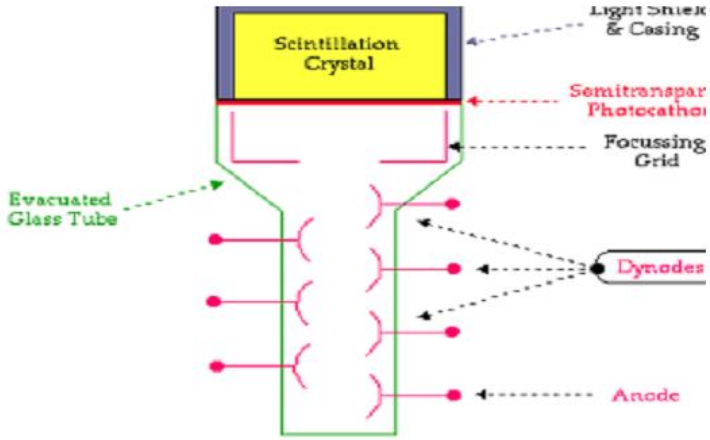

Figure (A-3)shape and structure of Photomultiplier Tube

The scintillation crystal, NaI (Tl) is very delicate and this is one of the reasons it is housed in an aluminum casing. The inside wall of the casing is designed so that any light which strikes it is reflected downwards towards the PMT. The function of the photocathode is to convert the light flashes produced by radiation attenuation in the scintillation crystal into electrons. The grid focuses these electrons onto the first

dynode and the dynode array is used for electron multiplication (usually 6 to 10). Finally the anode collects the electrons produced by the array of dynodes, (1, 2).

Position logic Circuitry

The position logic circuits immediately follow the photomultiplier tube array and they receive the electrical impulses from the tubes in the summing matrix circuit (SMC). This allows the position circuits to determine where each scintillation event occurred in the detector crystal.The photomultiplier tubes are divided into horizontal halves to obtain X+ and X- signals and vertical halves to obtain Y+ and Y- signals.Four summing matrix circuits are used to sum up for x+,x-,y+ and y- signals from each TM tubes where each of these signals is the product of signal amplitude and position factor.A separate summing circuit is used to sum up a total signal Z from all PM tubes (signal amplitude only, no position factor)

The radiation position is then determined by X=k(X+-X-)/Z and Y=k(Y+-Y-)/Z where k is a scale constant, Z is the total signal amplitude and proportional to the incoming radiation energy.The positional signals X and Y must be normalized by total signal Z because X and Y themselves depend on the both signal and positional factors (different radiation energy gives different signal amplitude at the same position)

Pulse Height Analysis

Is used to discriminate the amplitude of voltage pulses; A pulse height analyzer (PHA) consists of a lower level discriminator (which passes voltage pulses which are than its setting) and an upper level discriminator (which passes voltage pulses lower than its setting).

The result is a variable width window which can be placed anywhere along a spectrum, or used to scan a spectrum;

A single channel analyzer (SCA) consists of a single PHA with a scalar and a ratemeter;

A multi-channel analyzer (MCA) is a computer-controlled device which can acquire data from many windows simultaneously.

Data Analysis Computer

Finally, in order to deal with the incoming projection data and to process it into a readable image of the 3D spatial distribution of activity within the patient, a processing computer is used. The computer may use various different methods to reconstruct an image, such as filtered back projection or iterative reconstruction, both of which are further described in this tutorial.

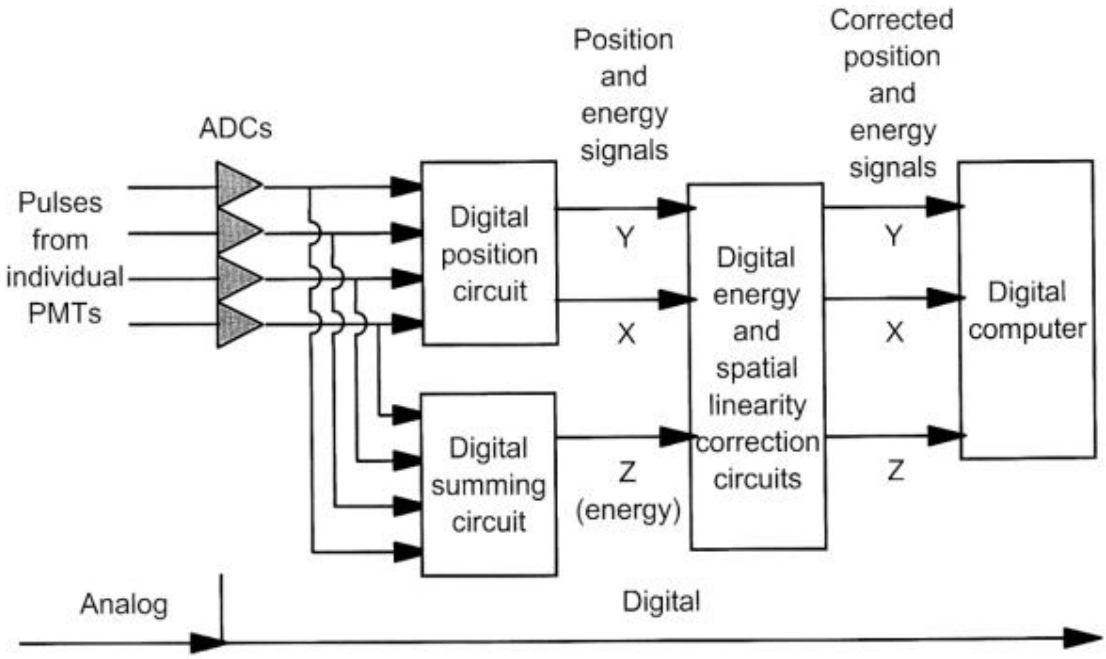

Figure (A-5) electronic circuit of a modern digital scintillation camera